北京航空航天大學
BEIHANG UNIVERSITY

Theoretical and Experimental Studies of Atomic Oxygen Interacting with Material Surfaces in Low Earth Orbit

Chun-Hian Lee
Zhigang Shen
Laiwen Chen
Xiaohu Zhao

2006

1. Introduction
2. Experimental Studies of Atomic Oxygen Effects on Space Material Surfaces
3. Theoretical Modeling and Numerical Simulation
4. Concluding Remarks

I. INTRODUCTION

- **Space environment:**
  - **Highly complex**
  - **Altitude of 200~700 km (LEO):**

    atomic oxygen erosion – highly oxidative environment

    ultraviolet radiation

    vacuum ultraviolet radiation

AO in LEO

- **Pressure: 10^{-3} ~ 10^{-5} Pa**

  Photochemical reaction $O_2 + h\nu \rightarrow 2O$

- **Number density ~ O (10^9) cm^{-3}**
- **Spacecraft orbital velocity approx. 8 km/s**

  Actual flux of AO impinging on orbiting vehicle approx. : 10^{14} ~ 10^{15} atoms/cm^2-s

- **Impact energy of AO onto spacecraft surface: 4.4~4.5 eV $\pm$1.0 eV**

- Research on atomic oxygen effects on space materials at BUAA
  - Experiments
  - Numerical simulation

II. Experimental Studies of Atomic Oxygen Effects on Space Material Surfaces

2.1 Ground Test Facility for Simulating Space Environment

- Test facility for atomic oxygen effects
- Ultraviolet radiation system
- Vacuum ultraviolet radiation system

2.1.1 AOE (Atomic Oxygen Effects) Test Facility

1. A hot cathode filament discharge plasma-type facility

➢Consisting of several subsystems:

- Hot cathode filament discharge
- Surface-restrained multiple magnetic
- Parametric diagnostic subsystem

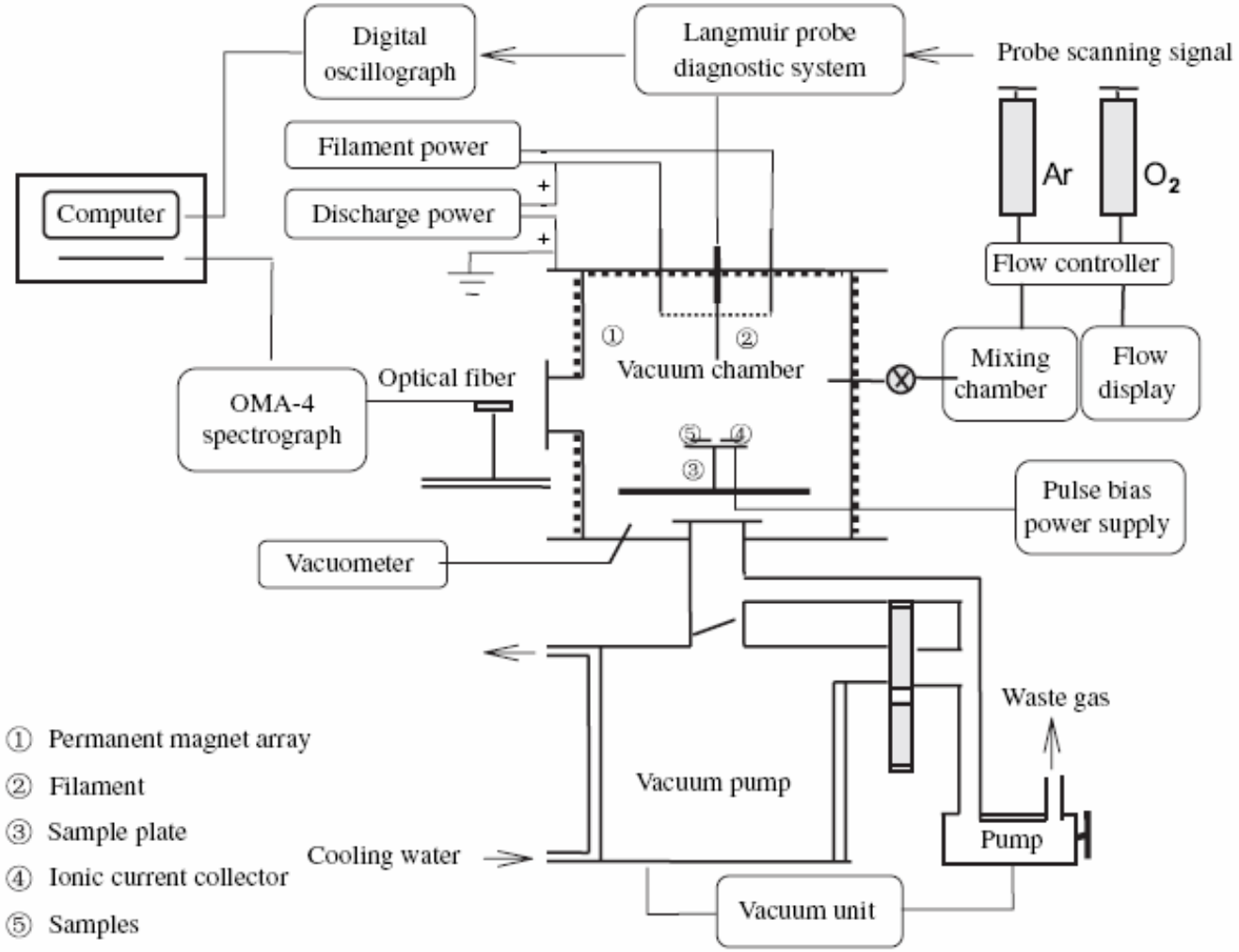
Digital oscillograph
Langmuir probe diagnostic system
Probe scanning signal
Filament power
Discharge power
Computer
Ar
O_2
Flow controller
①
②
Vacuum chamber
Mixing chamber
Flow display
OMA-4 spectrograph
Optical fiber
⑤
④
③
Pulse bias power supply
Vacuometer
Waste gas
Vacuum pump
Pump
Cooling water
Vacuum unit
① Permanent magnet array
② Filament
③ Sample plate
④ Ionic current collector
⑤ Samples

2. Main components of the plasma:

$$O_2, O_2^+, O, O^+, e$$

- **Flux of atomic oxygen 10^{17} atoms/(cm^2·s)**
- **Flux of oxygen ions 10^{14} ions/(cm^2·s)**

3. Large number of pairs (with opposite poles) of permanent magnets placed on the boundary of vacuum chamber to confine the plasma to increase the density of the electrons (10^{10}/cm^3).

The magnetic field will decay rapidly away from the wall so that the flow field will not be influenced.

4. Effective cross-section ~ Φ20cm

2.1.2 Ultraviolet radiation (UV) experimental system

- **Ultraviolet radiation source: Deuterium lamp**

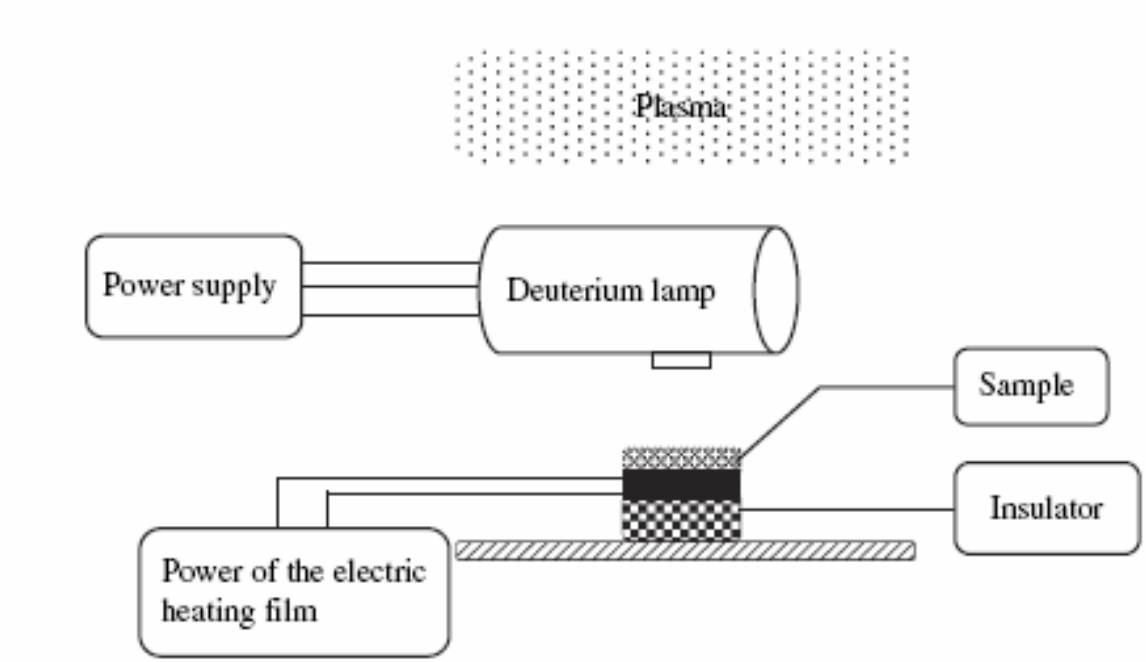

Schematic diagram of UV radiation Experimental system

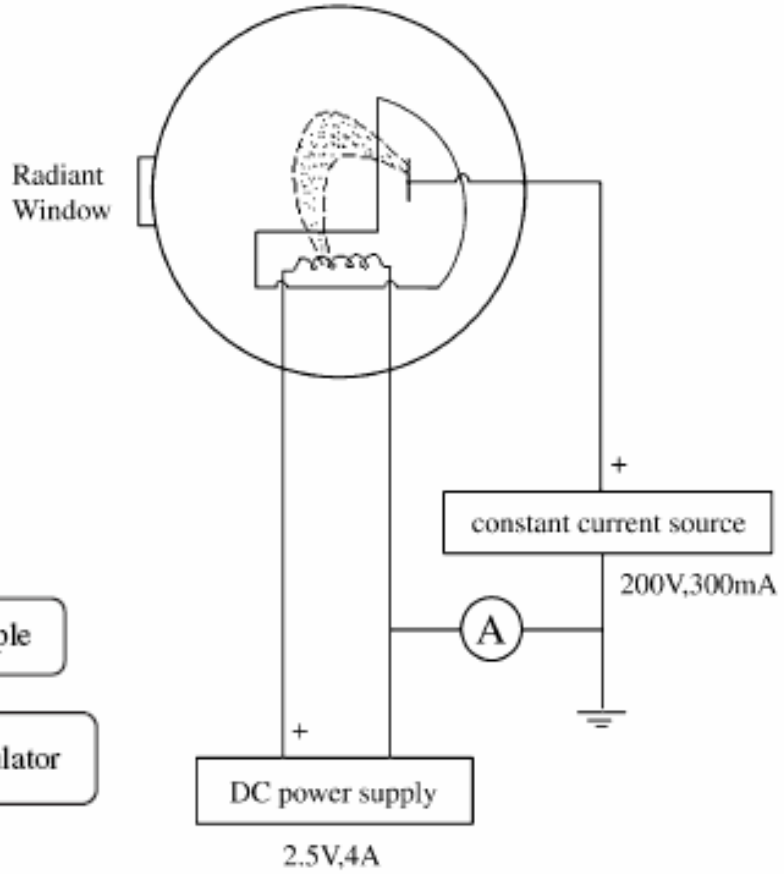

Working principle of deuterium lamp

Radiation spectrum of deuterium lamp

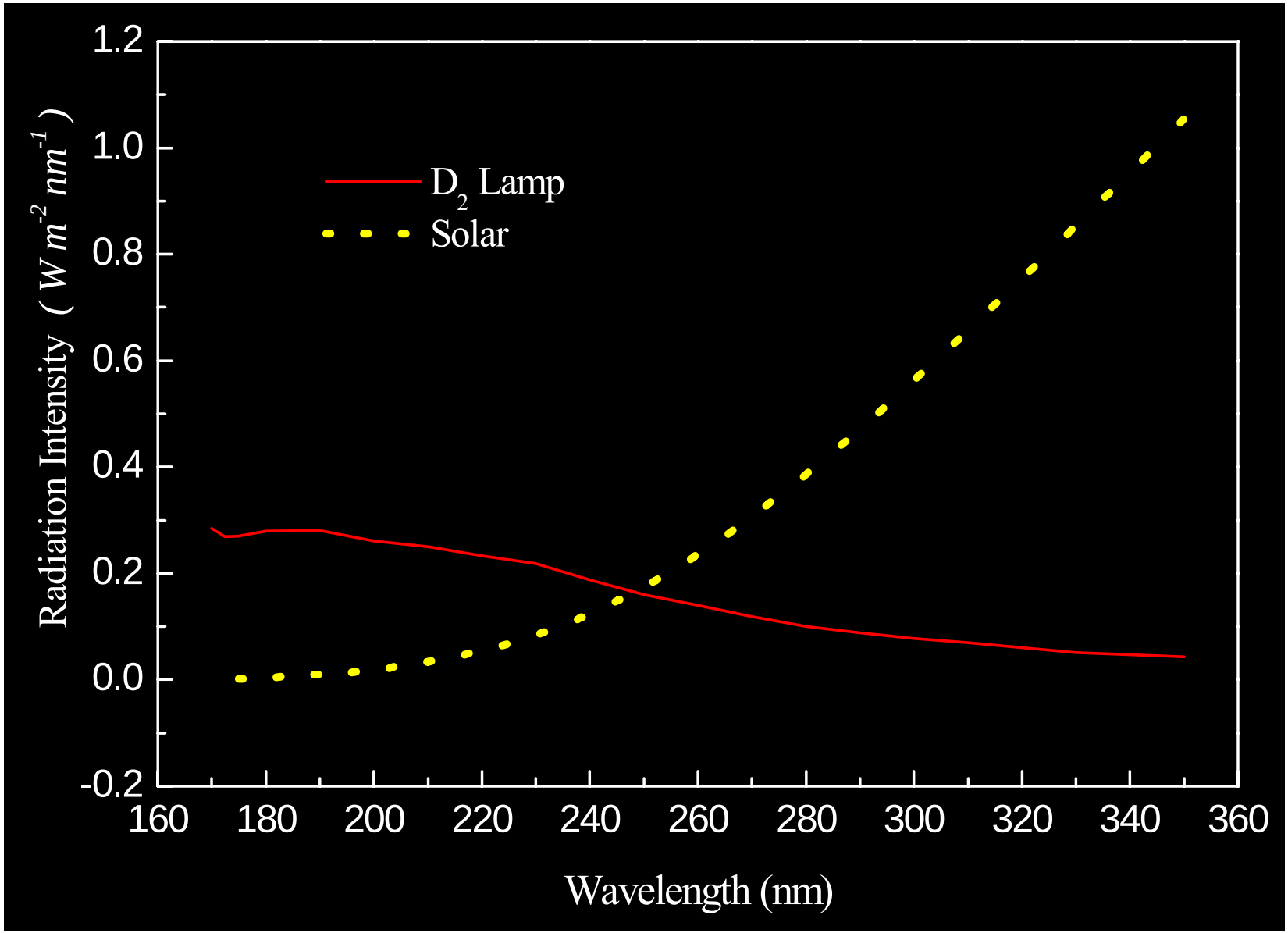

2.1.3 Vacuum ultraviolet radiation (VUV) Experimental system

- **Vacuum ultraviolet radiation source: Krypton lamp**

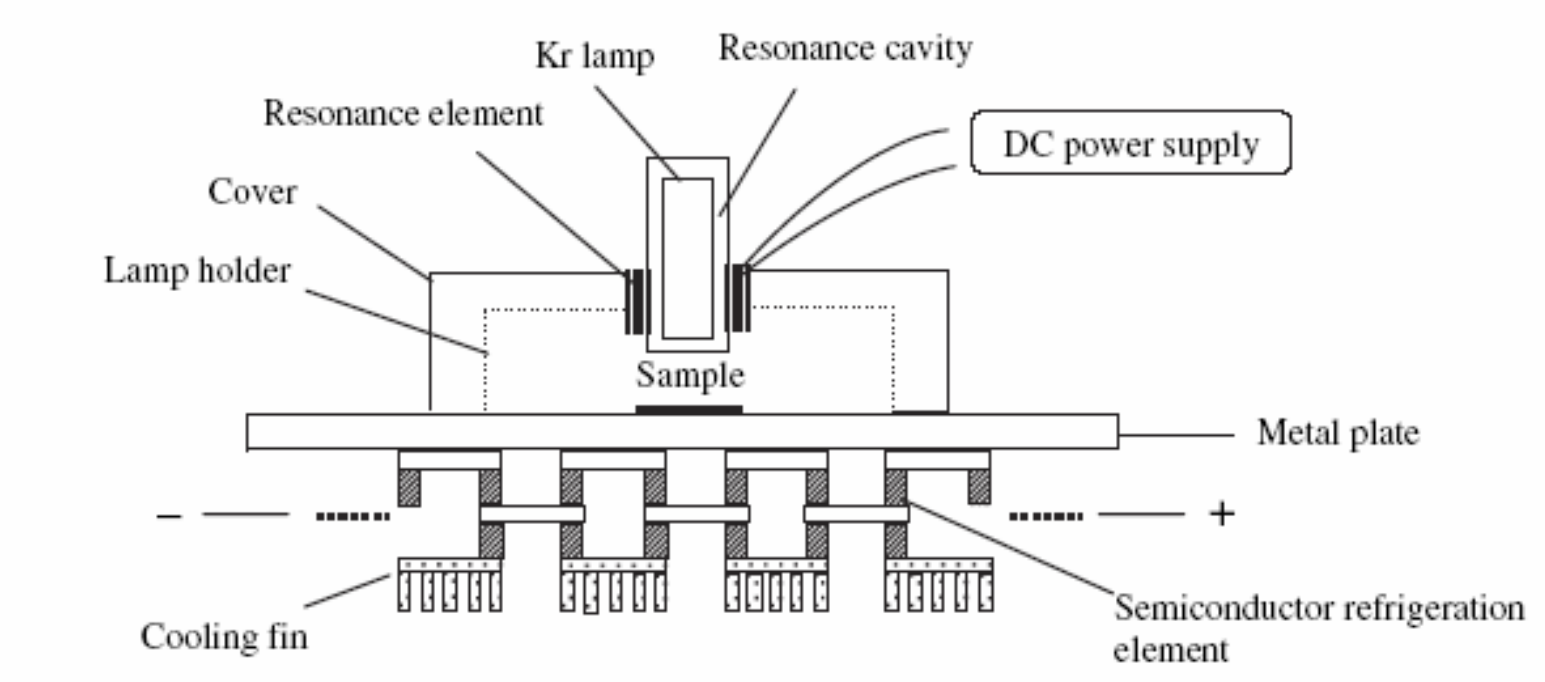

Schematic diagram of VUV radiation experimental system

Operational parameters:

- wave length ~ 123.6nm, within the range of 121.6nm (space) and 130nm (ground)
- no. of photons: 5×10^{14} photons/(cm^2·s)
  >> 4×10^{11} photons/(cm^2·s) (VUV strength in space)

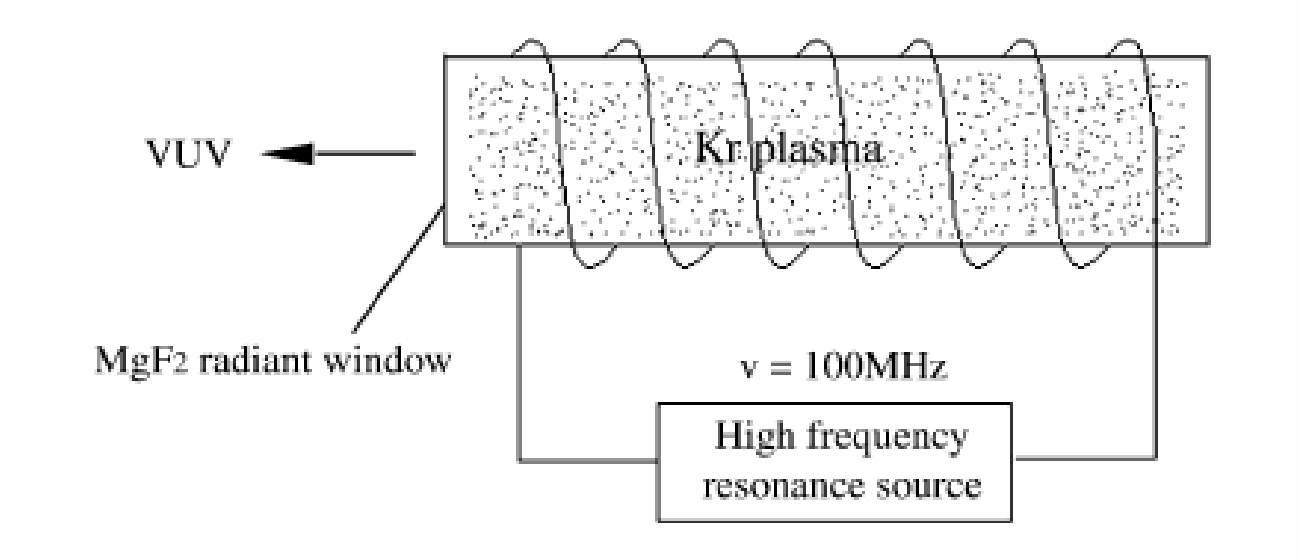

Operating principle schematic diagram for krypton lamp

2.2 Effects of Atomic Oxygen on Space Materials

2.2.1 Polymeric Materials

1. Kapton

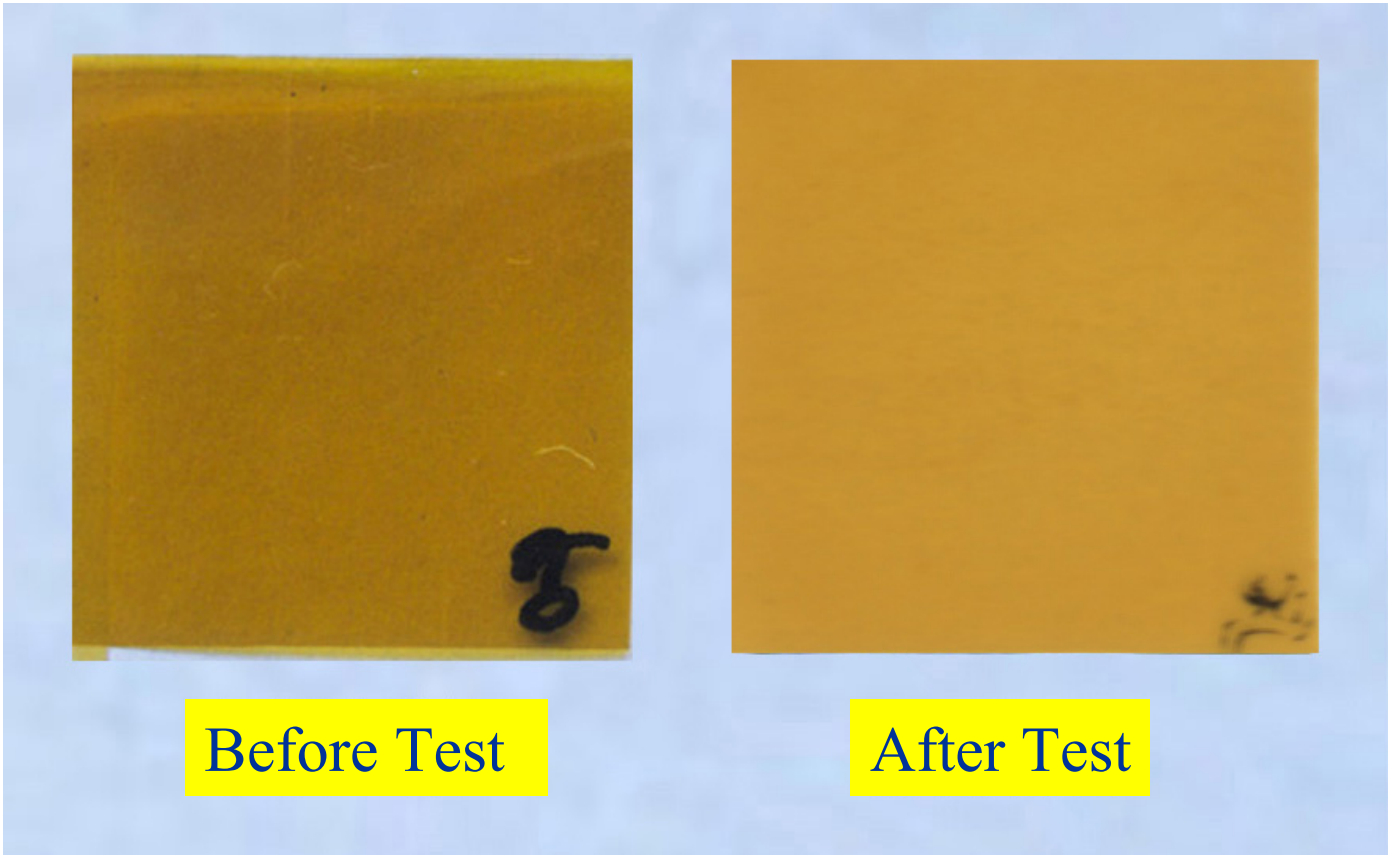

Scanning-electron-microscopic pictures of Kapton before and after AO exposure

erosion under moderately large AO flux

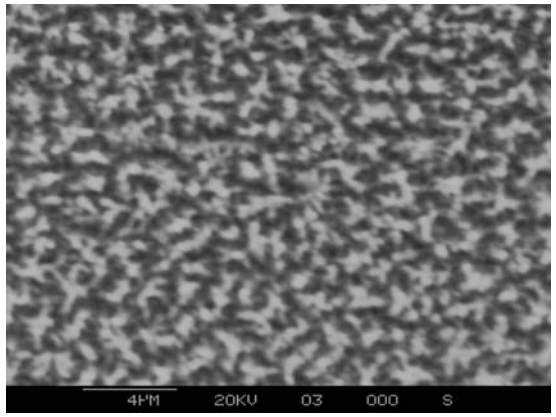

erosion under large AO flux

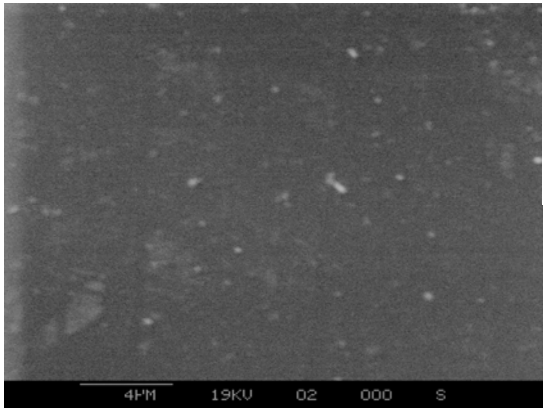

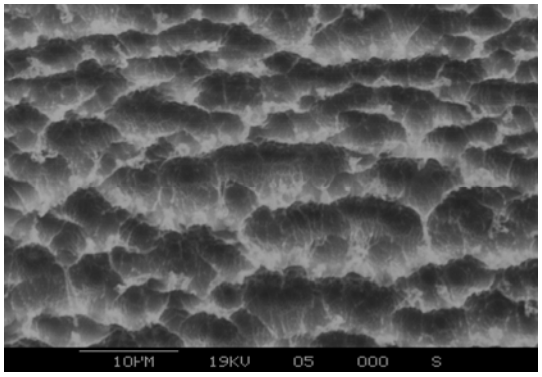

Optical parameters of Kapton (pre- and aft-tests)

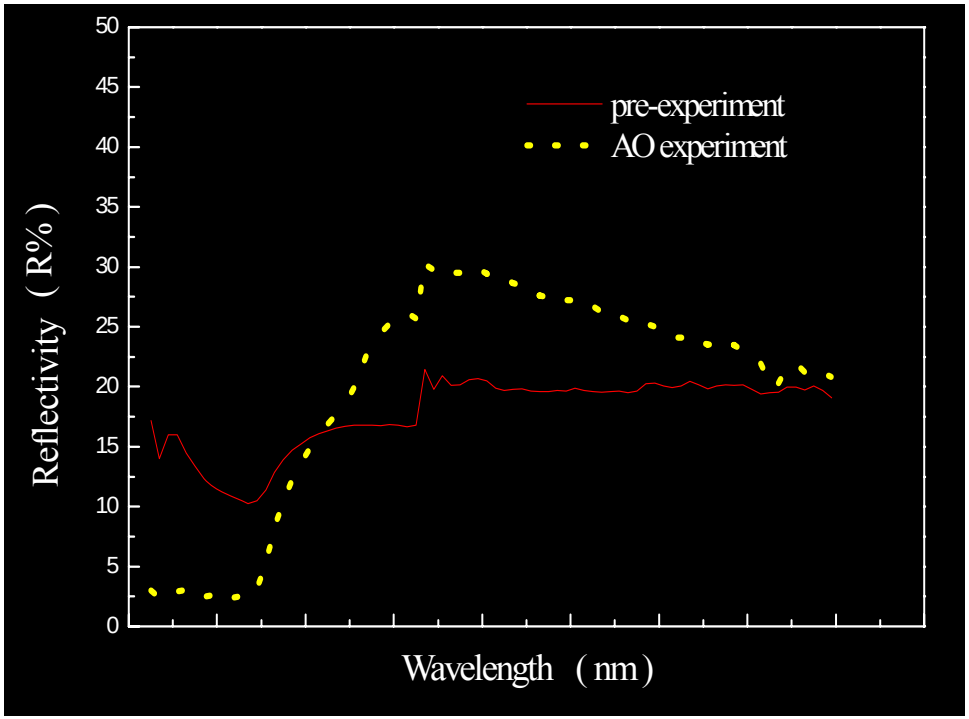

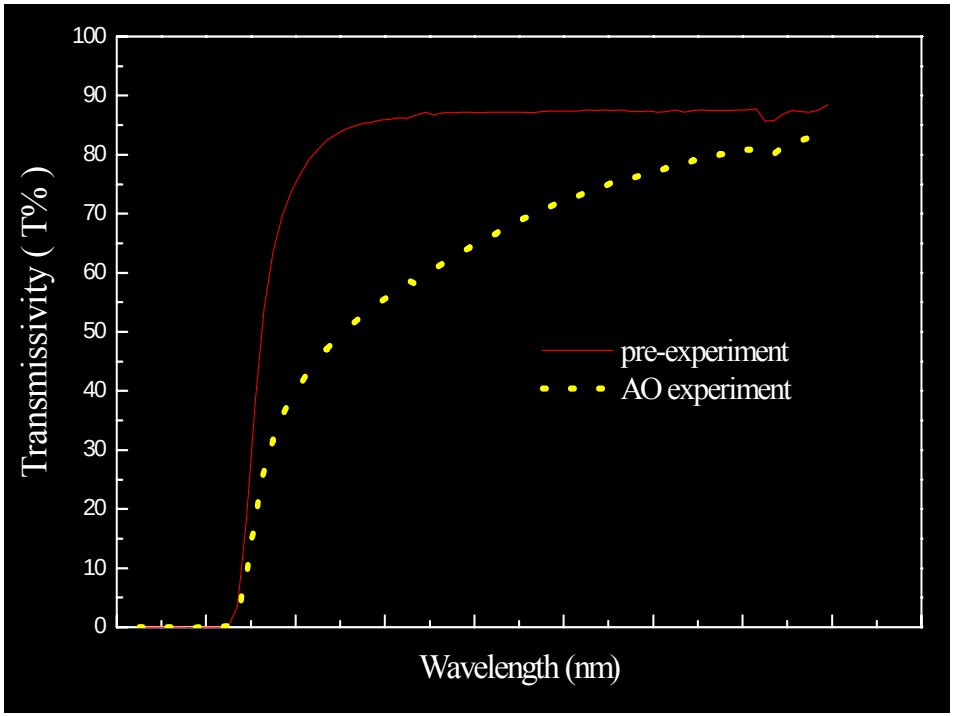

2. Teflon

- The appearance and optical parameters unchanged

SEM pictures of Teflon before and after AO exposures

Erosion due to low AO flux

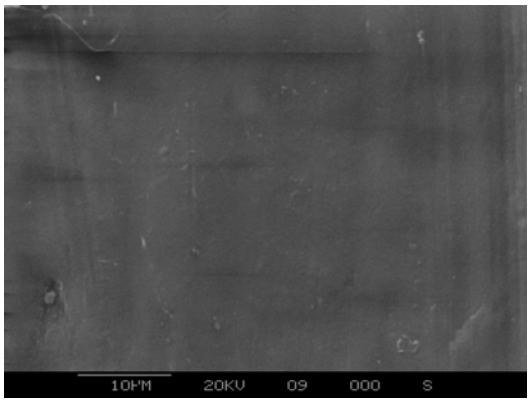

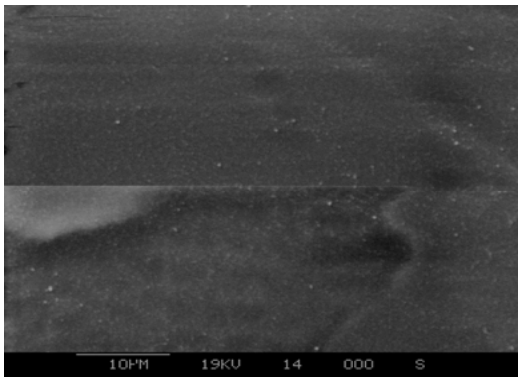

Erosion due to high AO flux

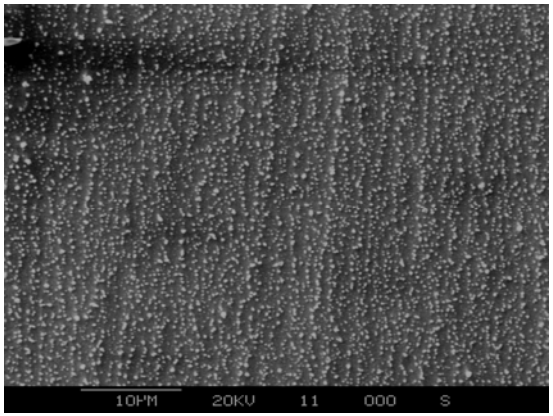

Mass loss and erosion of Teflon after AO exposures

Experiment	(1)	(2)
AO Fluence / atoms/cm^2	3.34×10^{20}	3.07×10^{20}
Mass Loss / g	0.01090	0.00980
Erosion Yield / cm^3/atom	2.96×10^{-24}	2.89×10^{-24}
Average Erosion Yield / cm^3/atom	2.93×10^{-24}	
Space Flight Results / cm^3/atom	$0.03\sim0.5\times10^{-24}$	
Ground-based Experiment Results of others / cm^3/atom	1.33×10^{-24}, 1.9×10^{-24}, $0.8\sim4.77\times10^{-24}$	

2.2.2 Composite Materials

1. β cloth

SEM pictures of β cloth before and after AO exposure

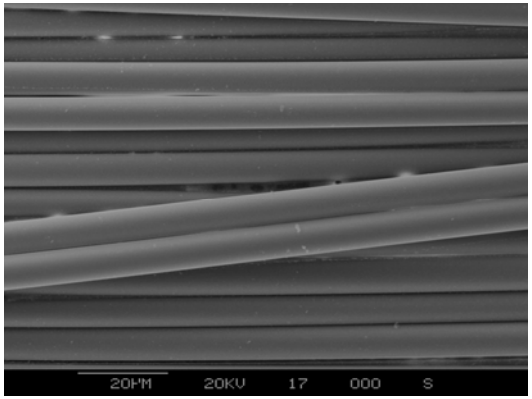

1000×

Erosion due to low AO flux

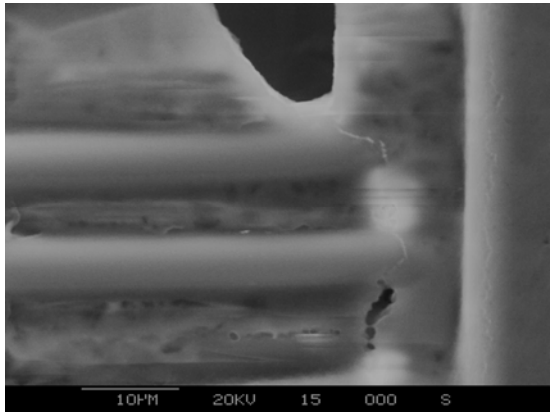

2000×

Erosion due to high AO flux

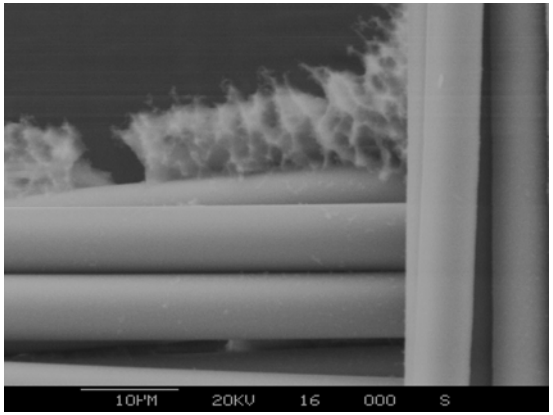

2000×

Mass losses and erosion rate of β cloth after AO

Experiment	(1)	(2)
AO Fluence / atoms/cm^2	3.34×10^{20}	3.07×10^{20}
Mass Loss / g	0.00395	0.00355
Erosion Yield / cm^3/atom	2.19×10^{-24}	2.24×10^{-24}
Average Erosion Yield / cm^3/atom	2.22×10^{-24}	

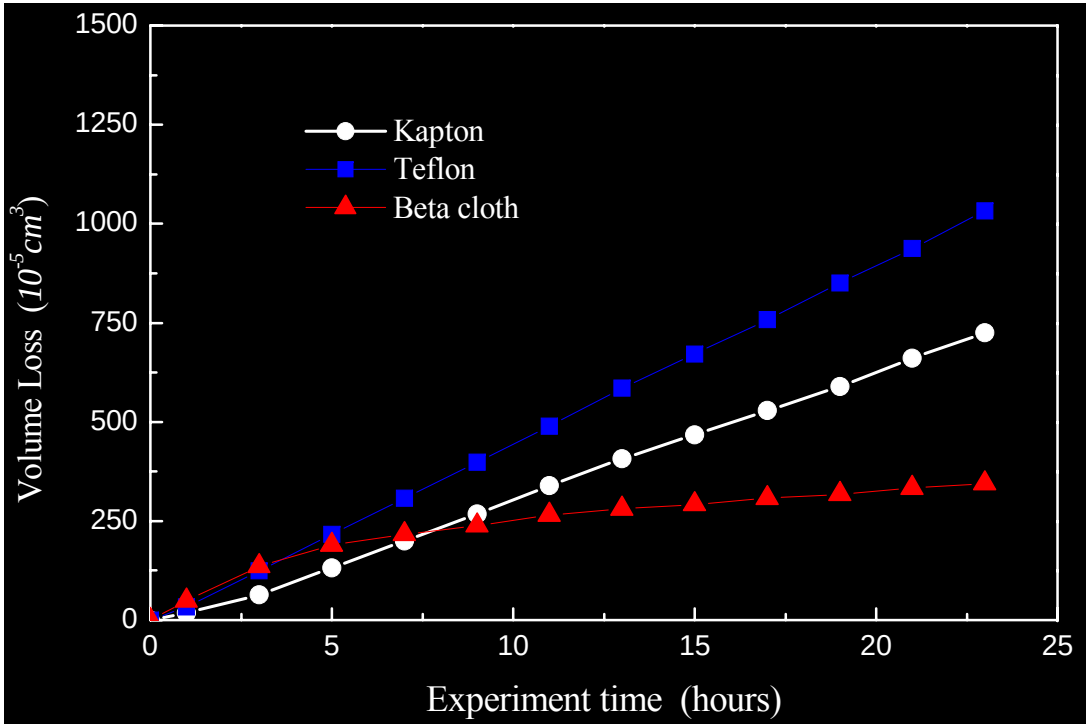

Volumetric losses of Kapton, Teflon, and β cloth in AO tests

2. Glass Fiber/Epoxy

SEM pictures of glass fiber/epoxy before and after AO exposure

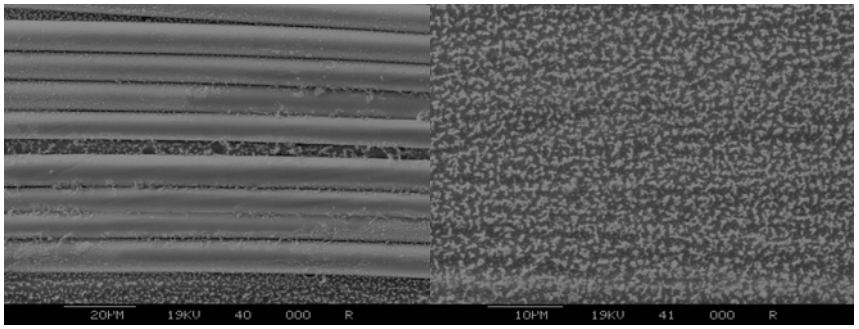

Fibers

Epoxy

Erosion due to low AO flux

Erosion due to high AO flux

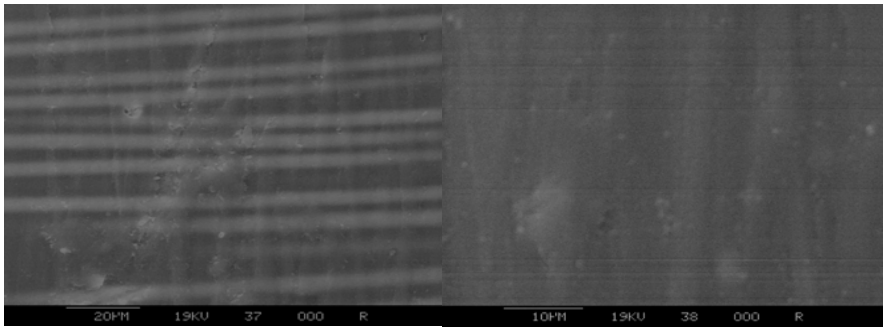

Fibers

Epoxy

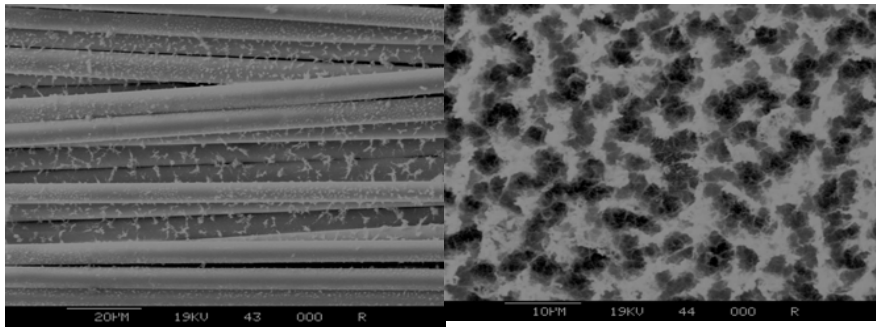

Fibers

Epoxy

Mass losses and erosion rate of glass fiber/epoxy after AO exposure

Experiment	(1)	(2)	(3)
AO Fluence / atoms/cm^2	2.80×10^{20}	1.96×10^{20}	1.96×10^{20}
Mass Loss / g	0.00365	0.00260	0.00270
Erosion Yield / cm^3/atom	1.84×10^{-24}	1.87×10^{-24}	1.94×10^{-24}
Average Erosion Yield / cm^3/atom	1.88×10^{-24}		

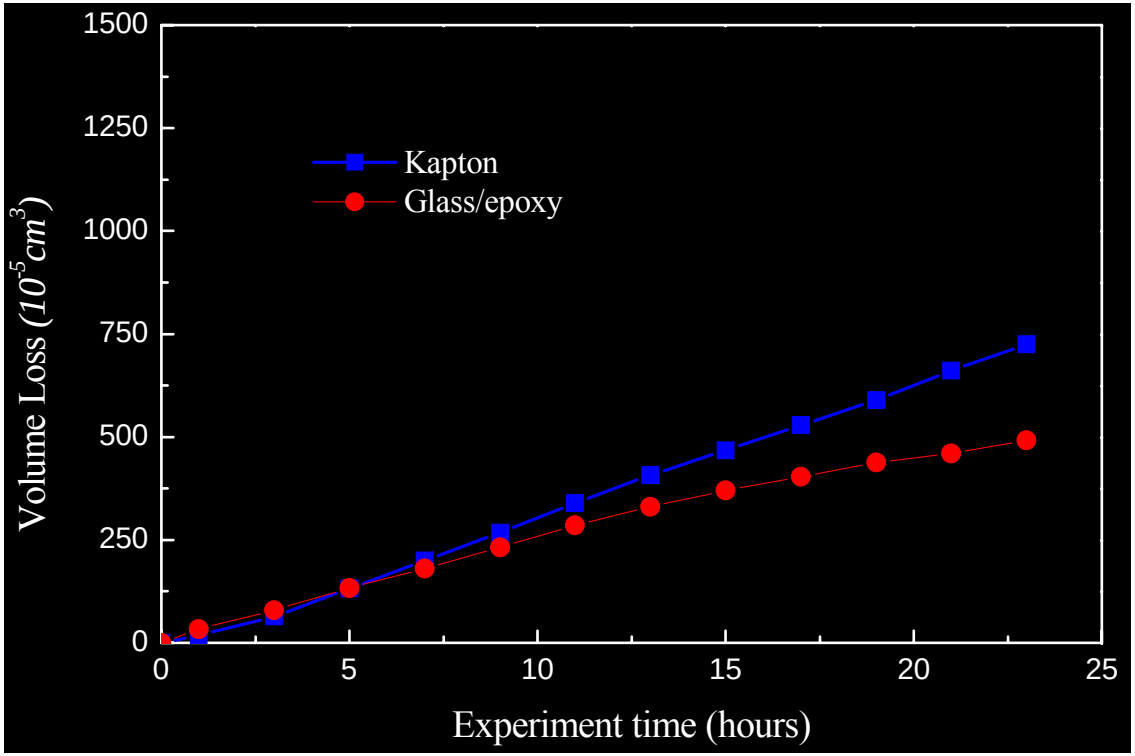

Volumetric losses of Kapton, and glass fiber/epoxy in AO tests

3. Carbon Fiber/Epoxy

SEM pictures of carbon fiber/epoxy before and after AO exposure

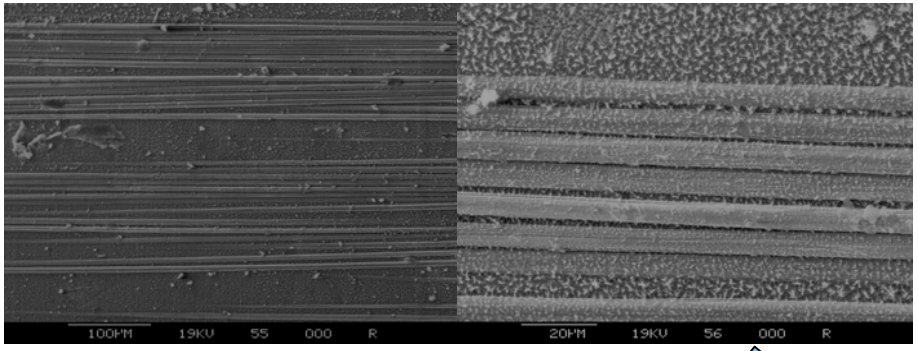

Erosion due to low AO flux

Erosion due to high AO flux

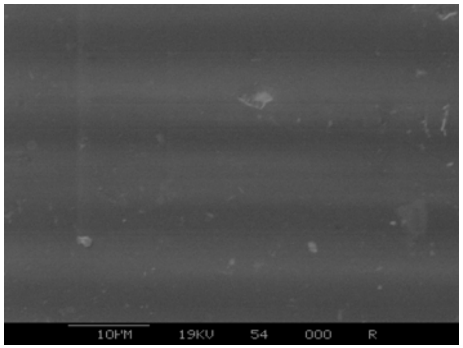

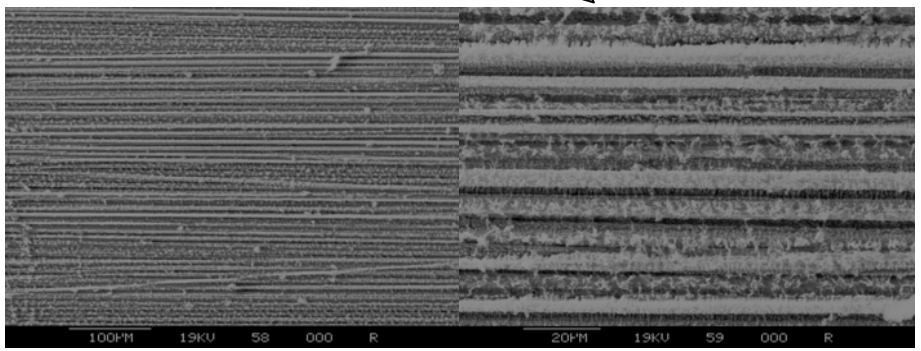

Mass losses and erosion rate of carbon fiber/epoxy after AO exposure

Experiment	(1)	(2)	(3)	(4)
Carbon fiber / Epoxy	T300/648		M40J/S-2	
AO Fluence / atoms/cm^2	1.96×10^{20}	3.27×10^{20}	1.96×10^{20}	3.27×10^{20}
Mass Loss / g	0.00235	0.00440	0.00310	0.00470
Erosion Yield / cm^3/atom	2.30×10^{-24}	2.28×10^{-24}	2.64×10^{-24}	2.58×10^{-24}
Flight Experiment Results / cm^3/atom	$2.1\sim2.6\times10^{-24}$			

2.3 Metal Silver Films

1. Appearance

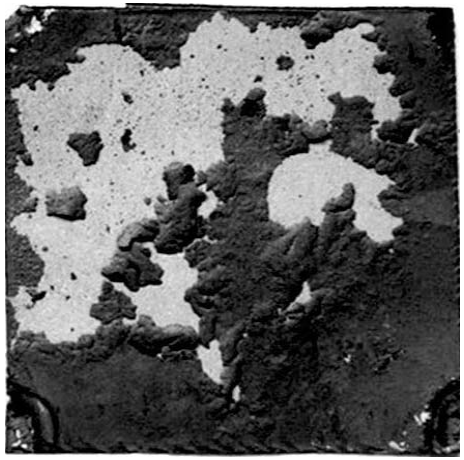

Erosion due to low AO flux

Erosion due to high AO flux

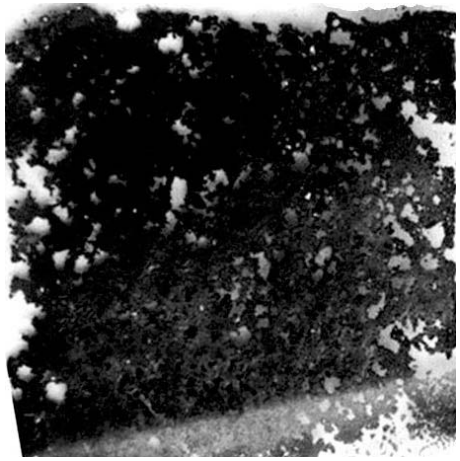

SEM pictures of silver film before and after AO exposure

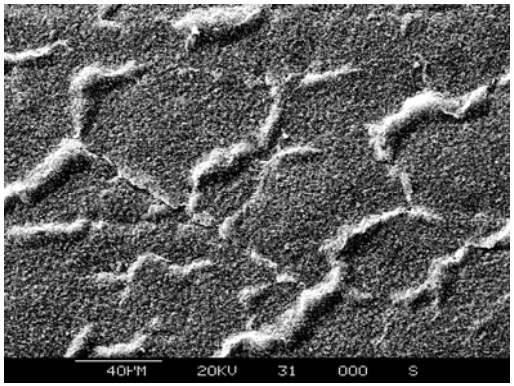

Erosion due to low AO flux

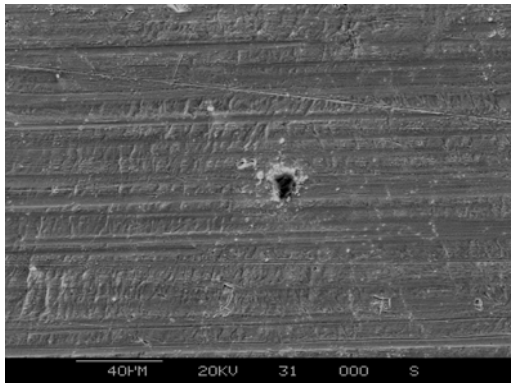

Erosion due to high AO flux

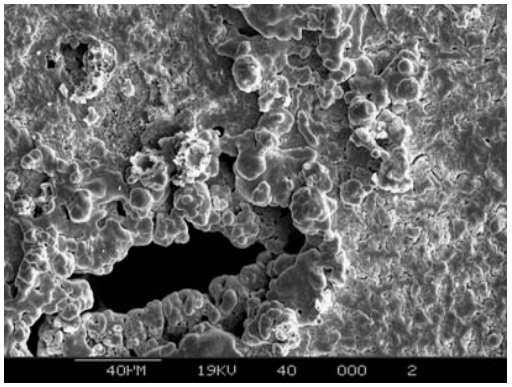

2.2 Coupled AO/UV/VUV Effects on Spacecraft Materials

1. Kapton

- Kapton would maintain its appearance, mass, surface characteristics and optical parameters unchanged under the action of UV and VUV radiation
- AO effects on Kapton maintain unchanged under the coupling UV /VUV effects

2. Teflon

Mass losses of Teflon after coupled AO/UV exposure

No.	(1)	(2)	(3)
Experiment	AO	AO	AO / UV
Temperature / °C	70	130	130
AO Fluence / atoms/cm^2	7.13×10^{19}		
Sample mass before experiment / g	0.09020	0.09225	0.10030
Sample mass after experiment / g	0.08525	0.08610	0.09410
Mass Loss / g	0.00495	0.00615	0.00620

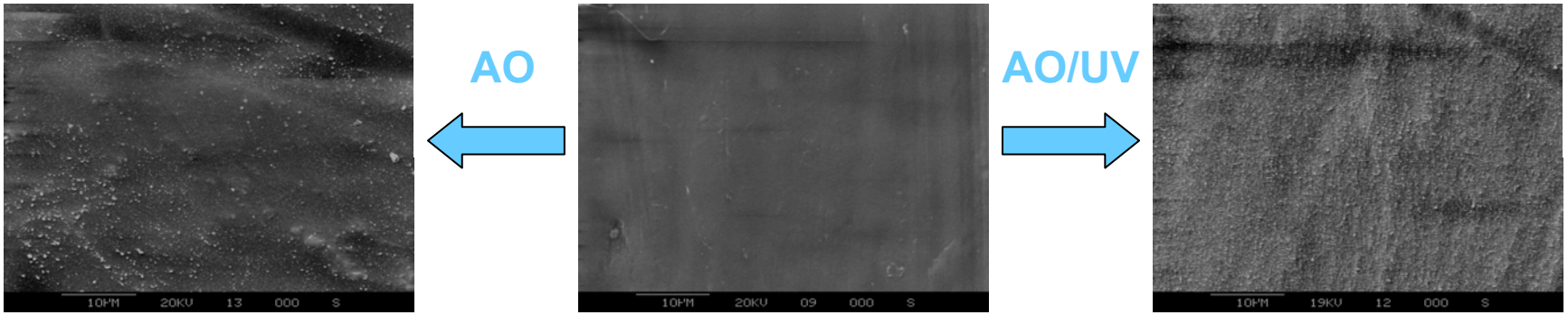

Appearance of Teflon before and after VUV radiation

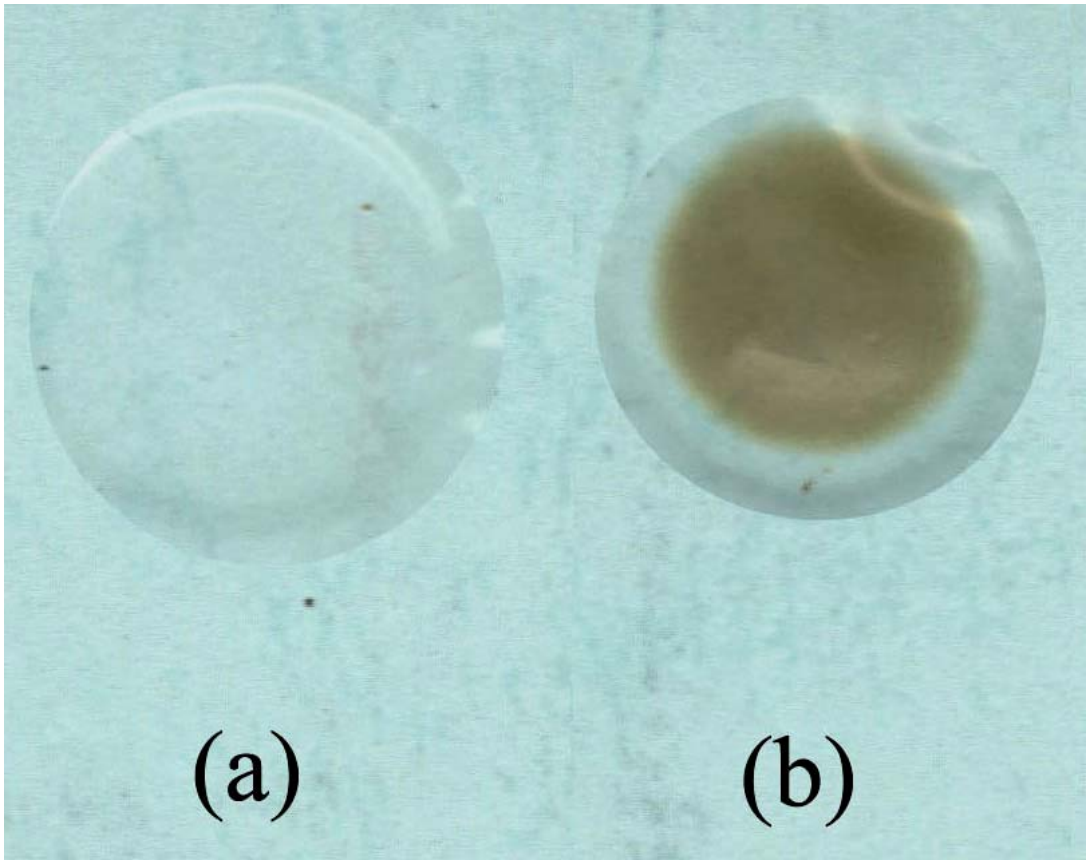

Optical parameters of Teflon before and after coupled VUV/VUV/AO exposure

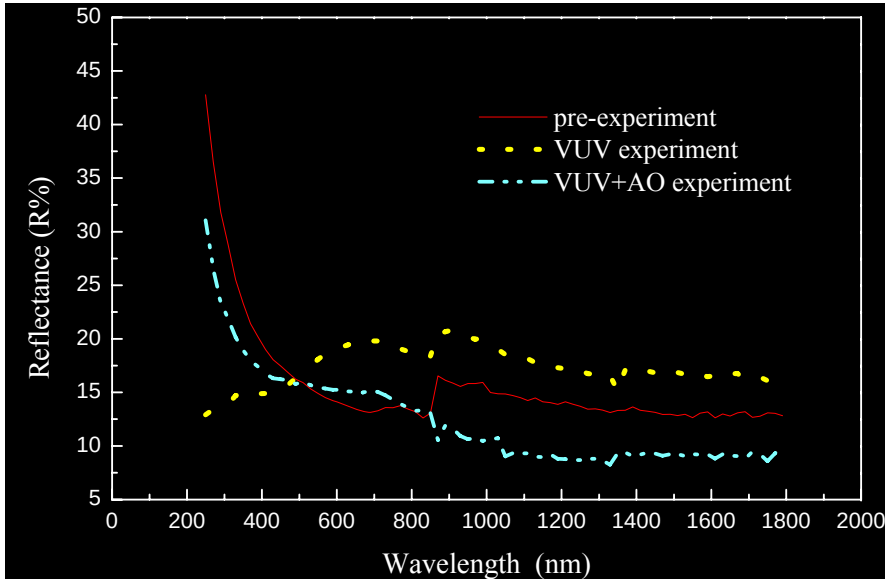

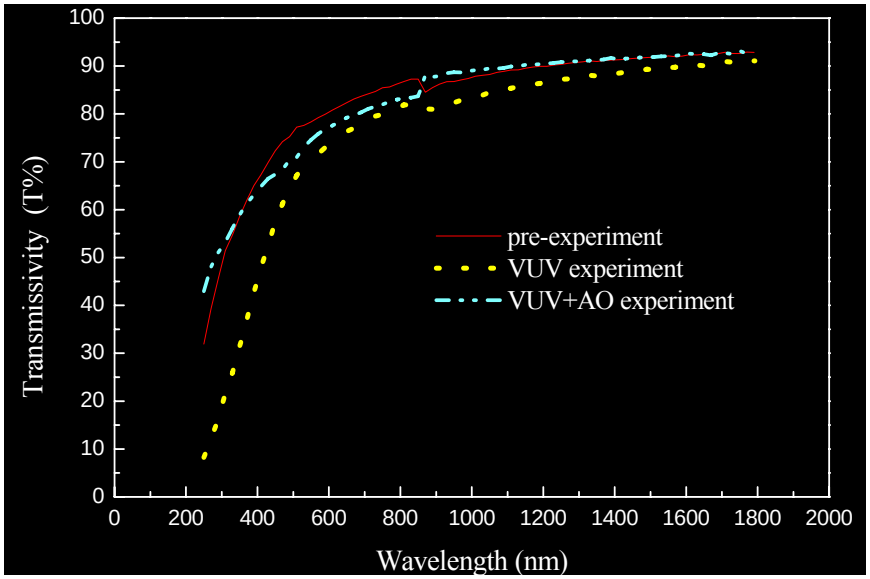

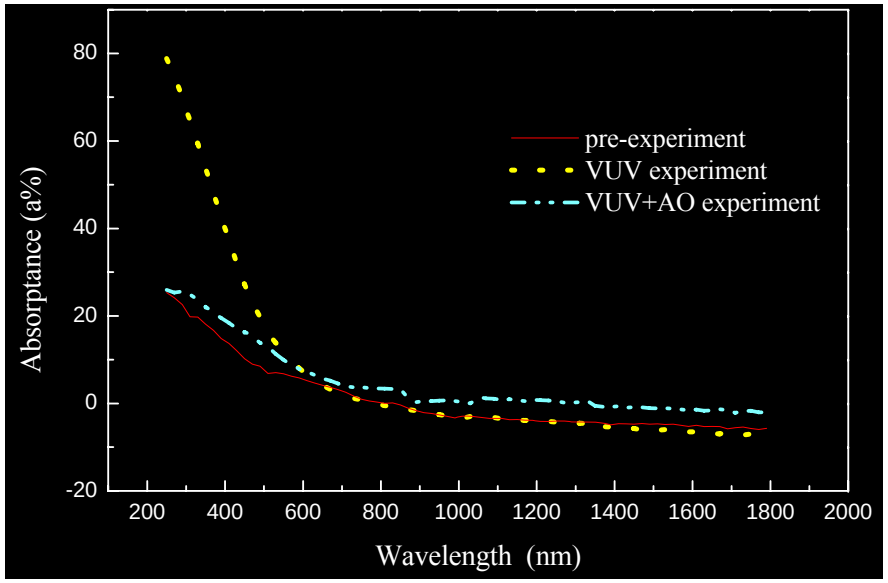

3. β cloth

Appearance of β cloth before and after VUV radiation

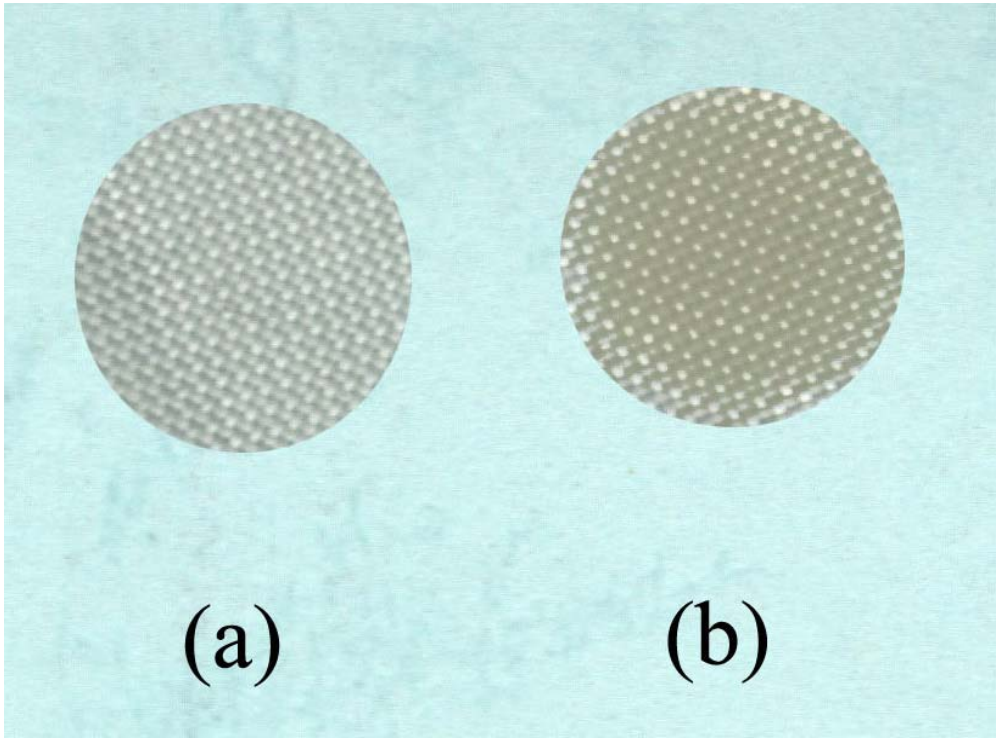

Optical parameters of β cloth before and after coupled VUV/VUV/AO exposure

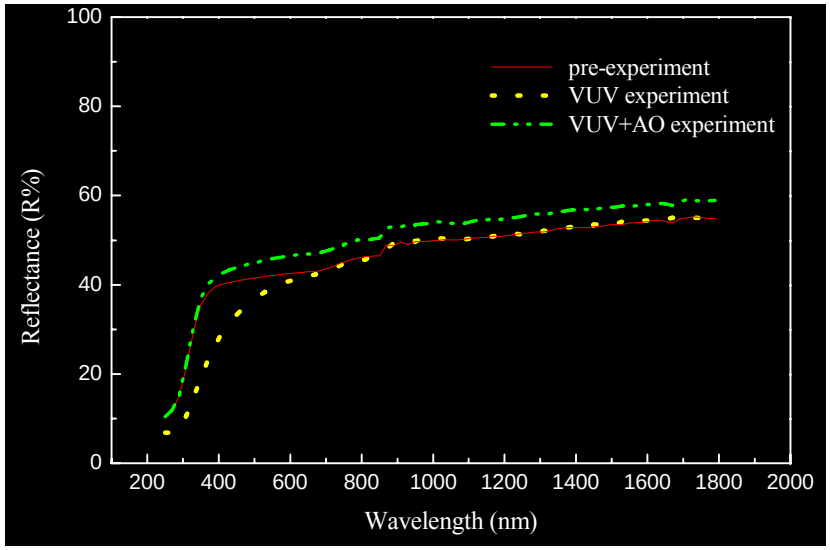

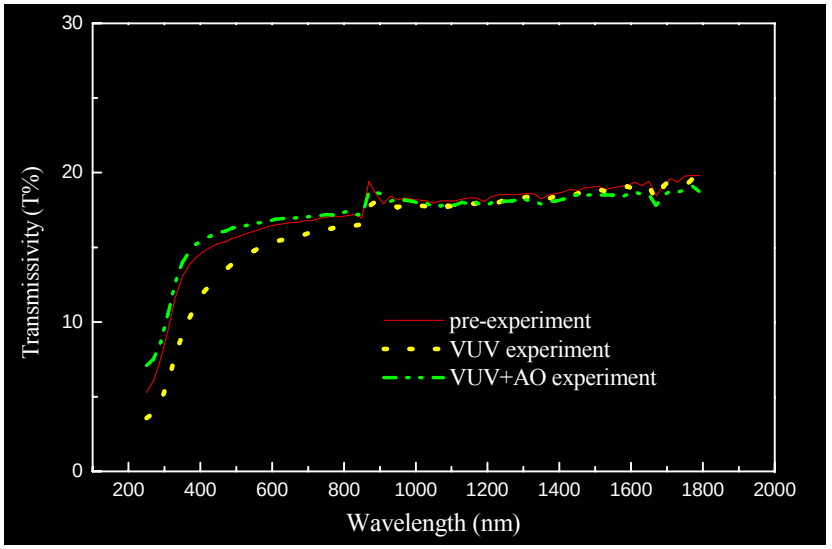

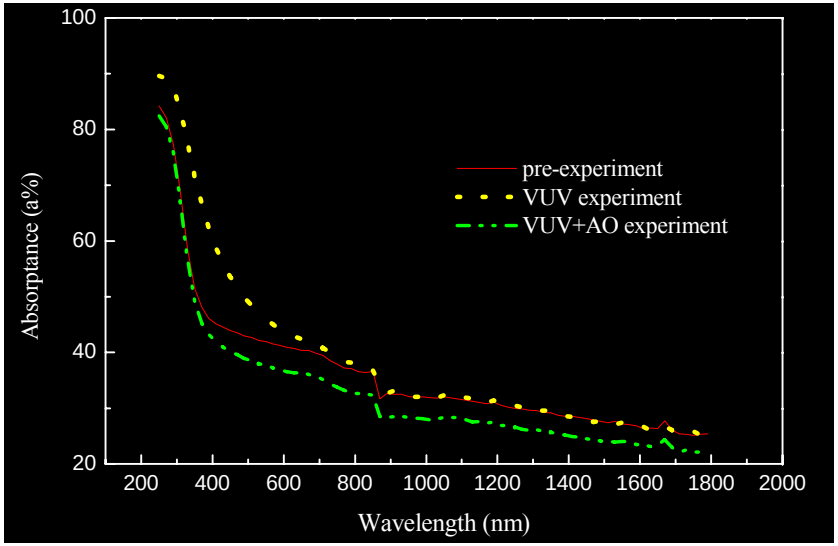

2.4 Anti-Erosion Study on Spacecraft Materials

2.4.1. Protection Coatings

- TO/Kapton
- Al/Kapton
- Au/Ag
- Pb-Sn/Ag

1. TO/Kapton

- Mass loss ~ 1/20 of Kapton

Erosion due to low AO flux

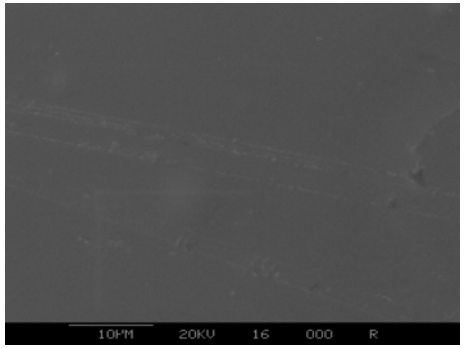

Erosion due to high AO flux

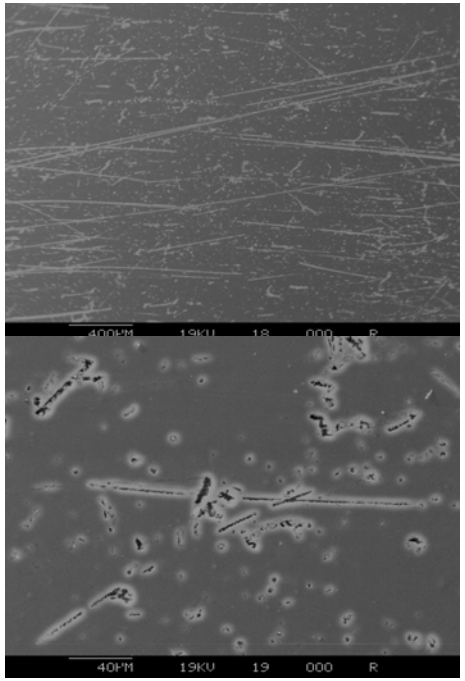

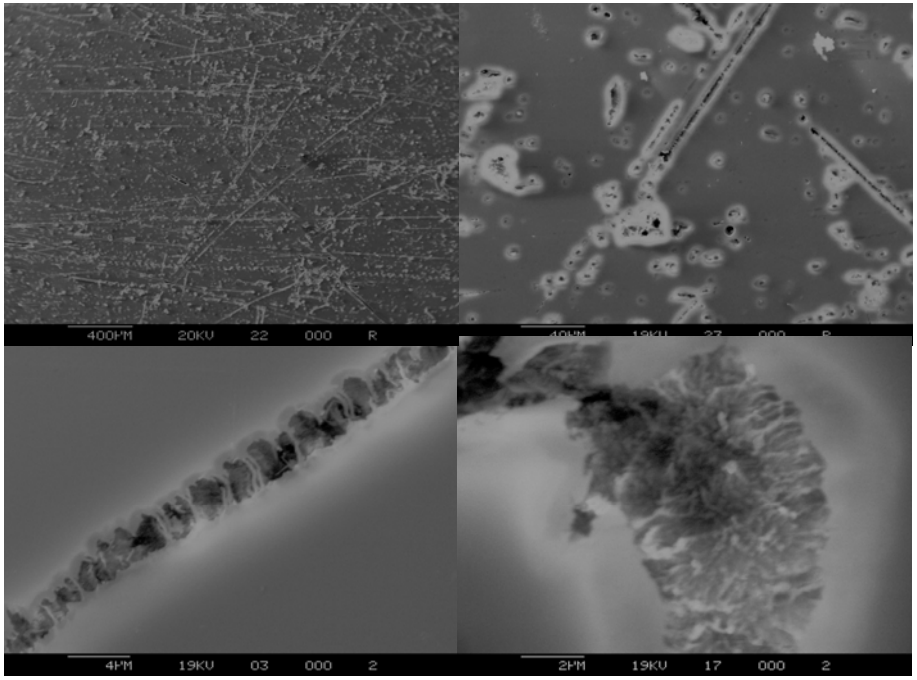

2. Al/Kapton

- Apperance, mass, and topographic nature are unchanged

3. Au/Ag Film

Mass losses of Au/Ag film after AO exposure

Experiment Sample	Ag	Au/Ag	
AO Fluence (atoms/cm^2)	4.11×10^{20}	4.11×10^{20}	4.11×10^{20}
Sample mass before experiment / g	0.09535	0.04835	0.04900
Sample mass after experiment / g	0.09595	0.04830	0.04900
The changes of sample mass / g	+ 0.00060	– 0.00005	0.0

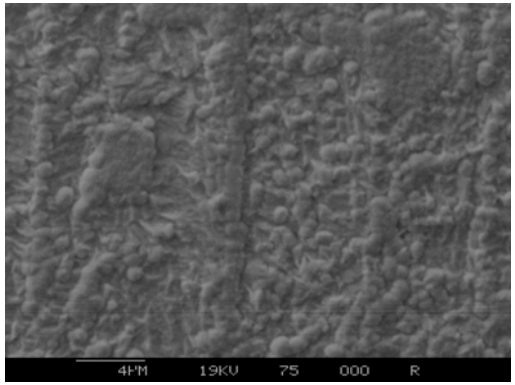

AO

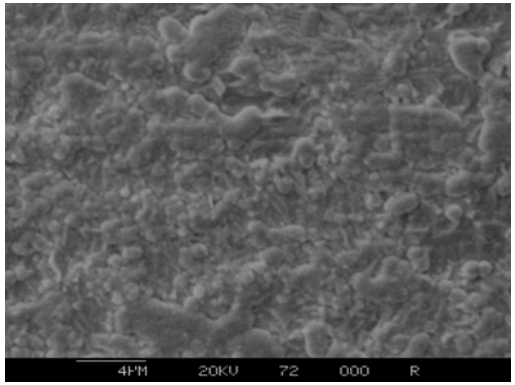

4. Pb-Sn/Ag

Mass losses of Pb-Sn/Ag film after AO exposure

Experiment Sample	Ag	Pb-Sn / Ag			
AO Fluence / atoms/cm^2	4.11×10^{20}	4.11×10^{20}		1.98×10^{21}	
Sample mass before experiment / g	0.09535	0.02920	0.03260	0.13520	0.14720
Sample mass after experiment / g	0.09595	0.02925	0.03260	0.13530	0.14720
The changes of sample mass / g	+ 0.00060	+ 0.00005	0.0	+ 0.00010	0.0

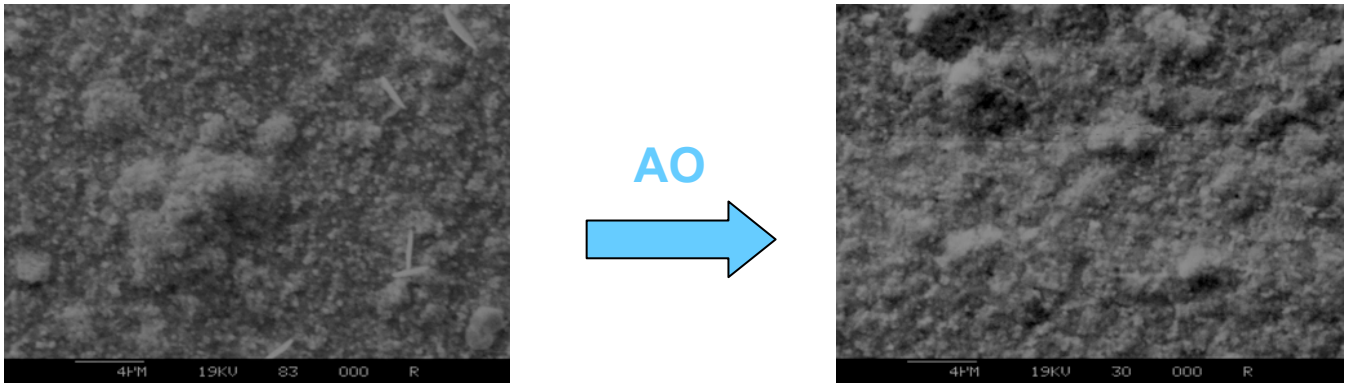

2.4.2 Compound with organic silicon additive

- KH560（3-Glycidoxypropyltrimethoxysilane）
- KH550（γ-Aminopropyl triethoxy silane）

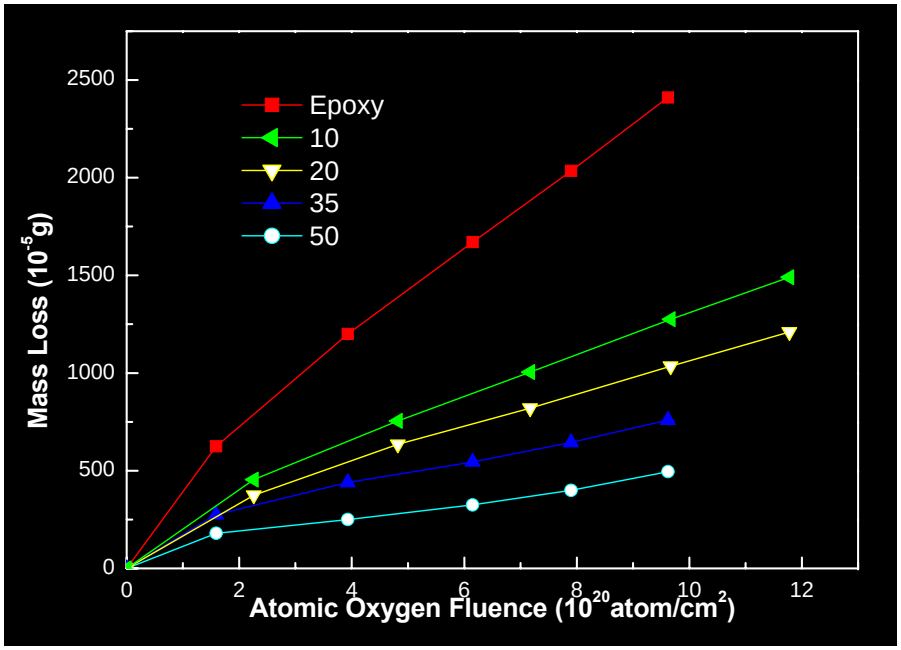

Mass loss of KH560/Epoxy

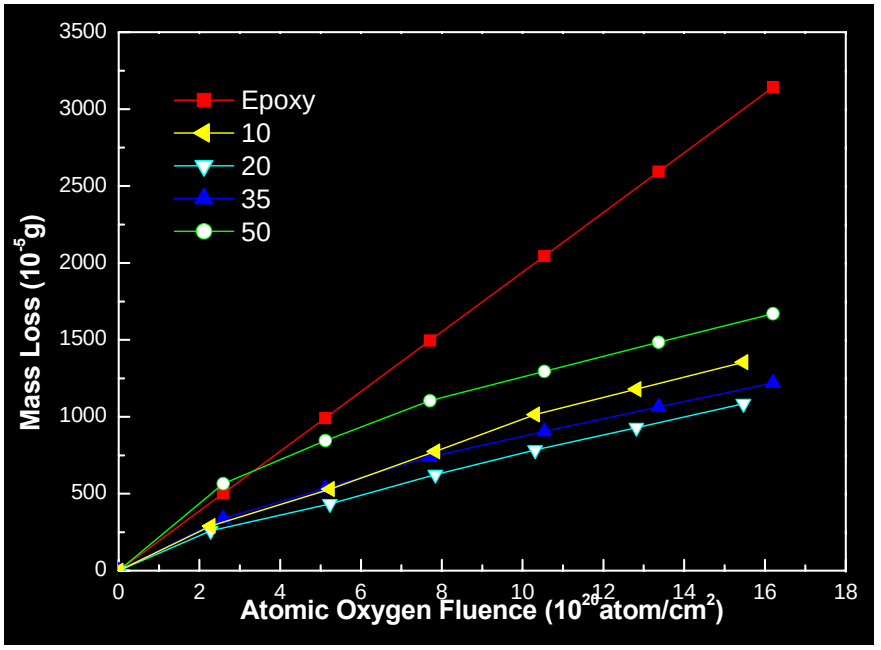

Mass loss of KH550/Epoxy

2.4.3 Inorganic Grain Additive Materials

1. Appearance before and after OA exposure

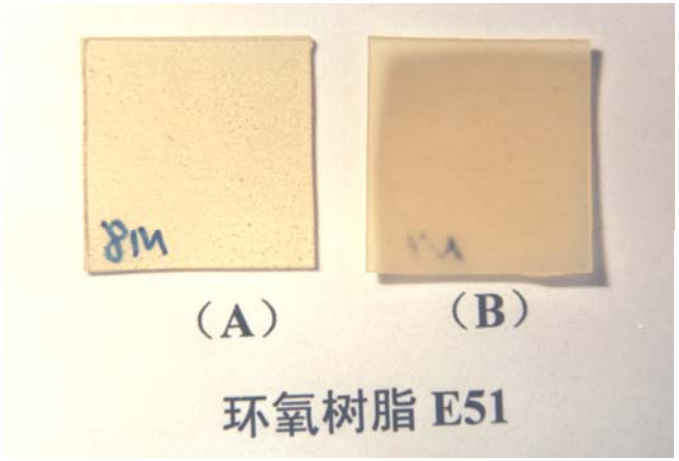

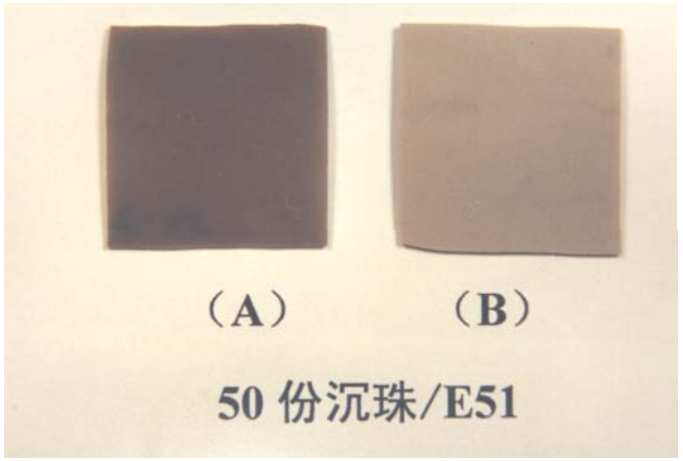

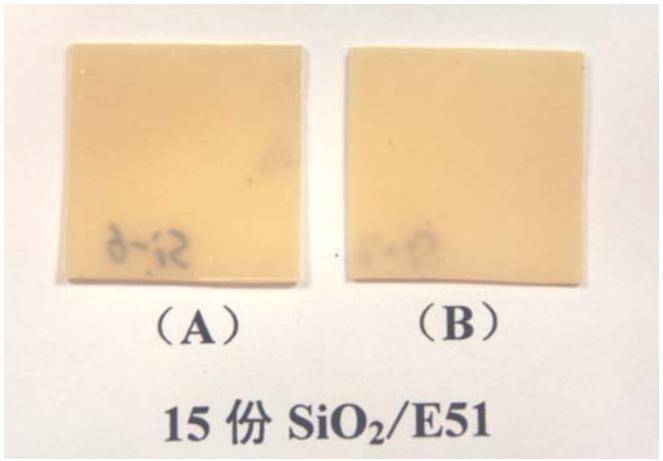

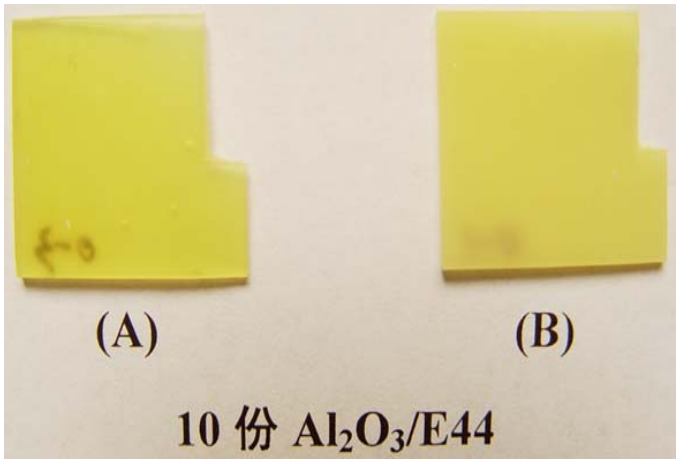

2. Mass loss after AO exposure

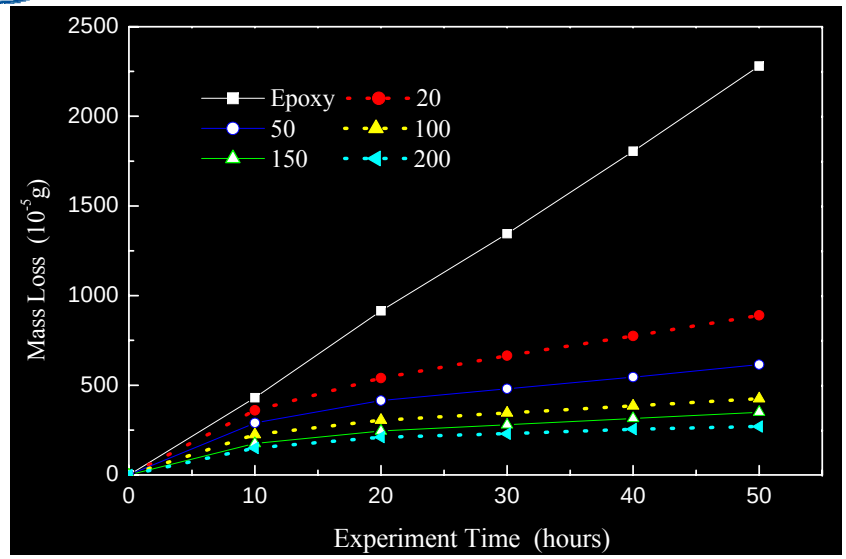

1. Ultrafined hollow grains（2μm）

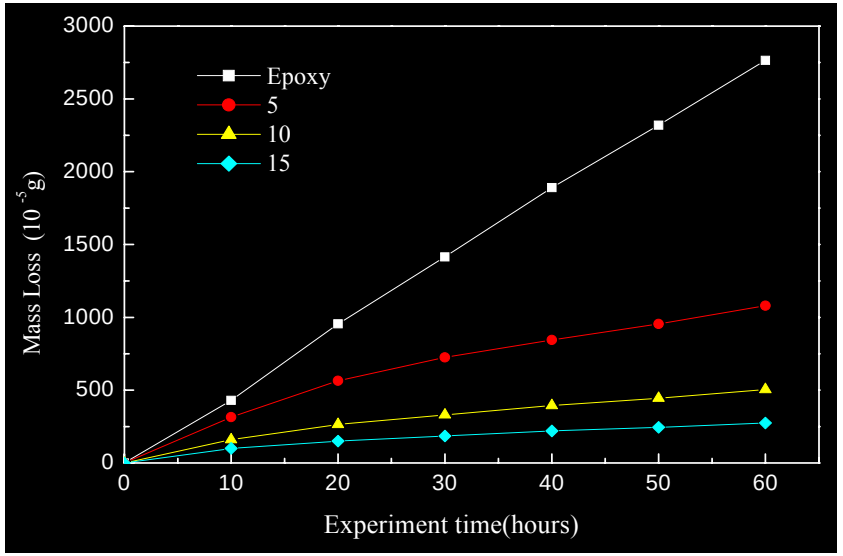

2. Nano-SiO_2（25nm）

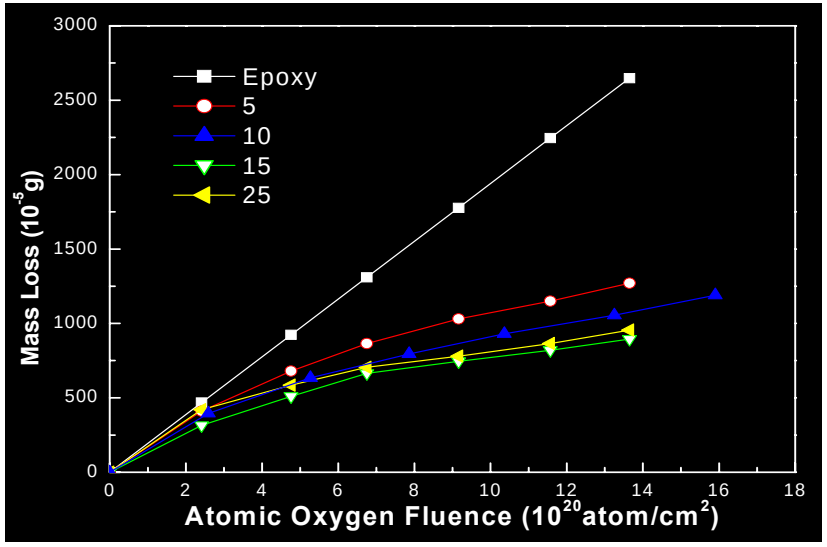

3. Nano-Al_2O_3（50nm）

3. Topographic characteristics of Material Surfaces

（1）Epoxy

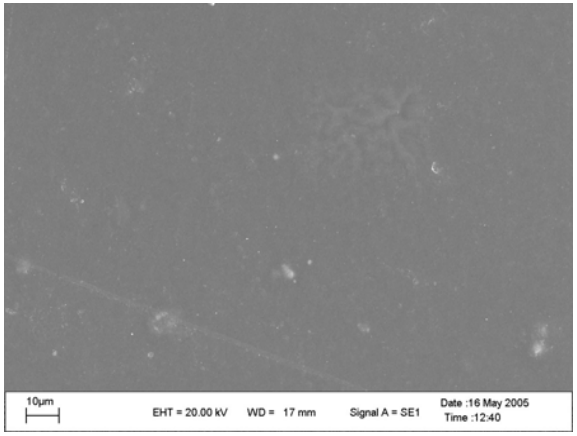

AO

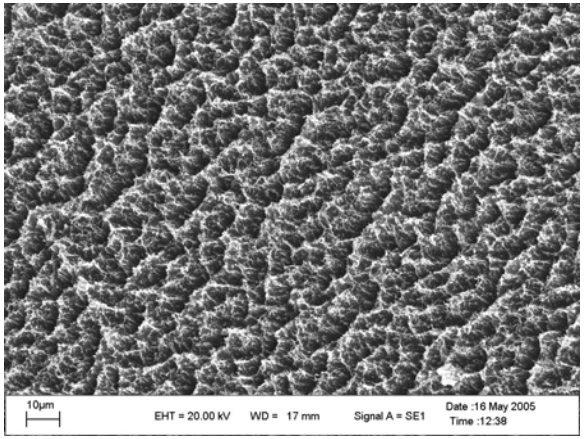

（2） Cenosphere/Epoxy

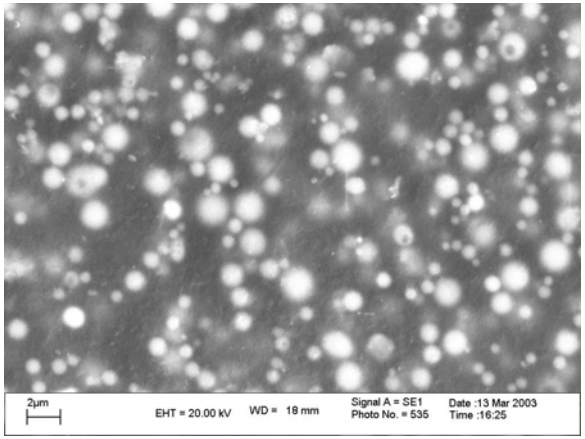

AO

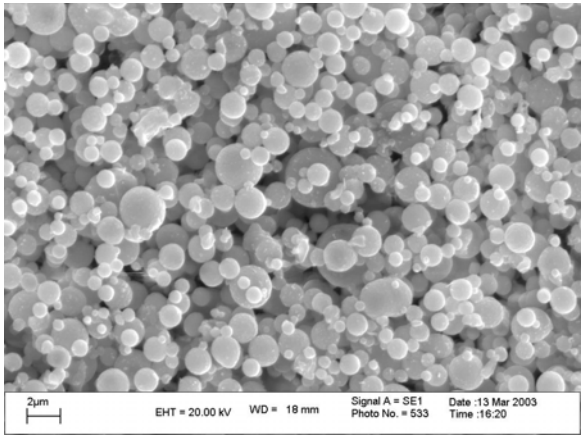

（3）SiO_2/Epoxy

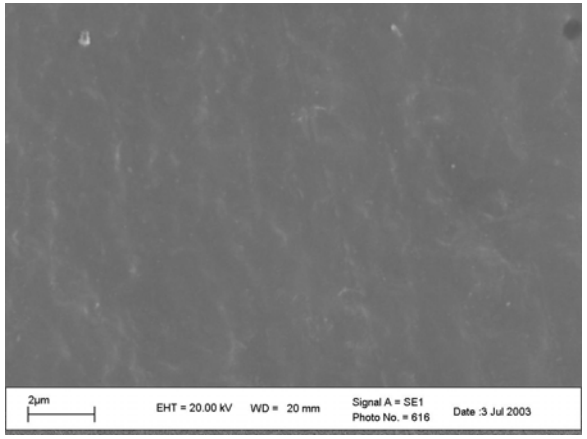

AO

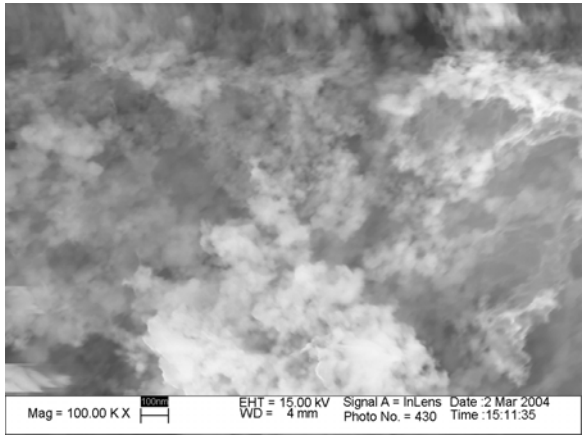

III. Theoretical Modeling and Numerical Simulation

3.1 Theoretical Model

- Dynamic Model
- Interaction Potential Model
- Reaction Probability Model

3.1.1 Dynamic Model

$$M_S d^2\boldsymbol{Y}_E/dt^2 = -\nabla_{\boldsymbol{Y}_E} V(\boldsymbol{X},\boldsymbol{Y}_I,\boldsymbol{Y}_E,\boldsymbol{Y}_F) - M_S\gamma d\boldsymbol{Y}_E/dt + \boldsymbol{f}_{\boldsymbol{Y}_E}(t)$$

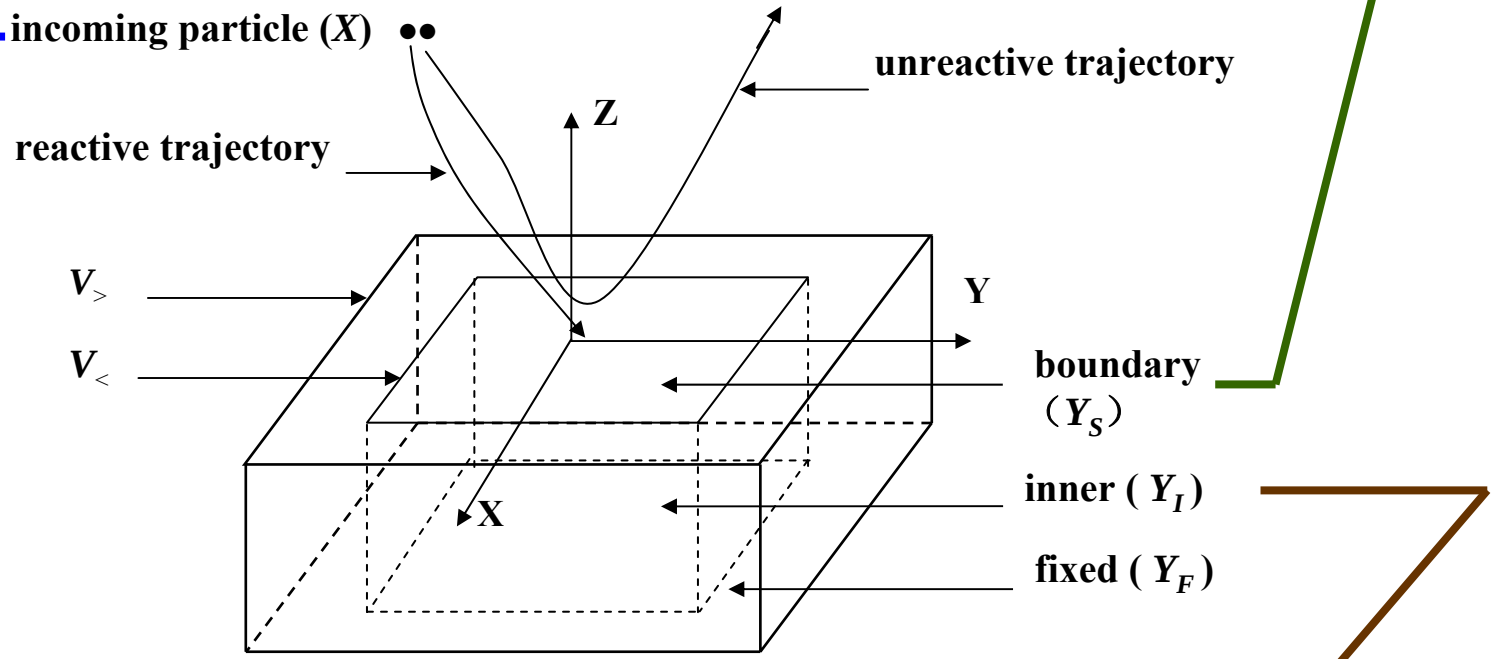

$$M_g d^2\boldsymbol{X}/dt^2 = -\nabla_{\boldsymbol{X}} V(\boldsymbol{X},\boldsymbol{Y}_I,\boldsymbol{Y}_E,\boldsymbol{Y}_F)$$

$$M_S d^2\boldsymbol{Y}_I/dt^2 = -\nabla_{\boldsymbol{Y}_I} V(\boldsymbol{X},\boldsymbol{Y}_I,\boldsymbol{Y}_E,\boldsymbol{Y}_F)$$

Geometric sketch of theoretical model

1. Dynamic Equations for Gas Particles

- **Free molecular flows**

$$M_g \ddot{\mathbf{X}} = -\nabla_{\mathbf{X}} V(\mathbf{X}, \mathbf{Y}_I, \mathbf{Y}_E, \mathbf{Y}_F)$$

2. Dynamic Equations for Particles in V< (*Inner Zone*)

- **Standard molecular dynamics**

$$M_S \ddot{\mathbf{Y}}_I = -\nabla_{\mathbf{Y}_I} V(\mathbf{X}, \mathbf{Y}_I, \mathbf{Y}_E, \mathbf{Y}_F)$$

3. Dynamic Equations for Particles in Edge Zone

- **Follow a class of Langevin equations**

$$M_S \ddot{\mathbf{Y}}_E = -\nabla_{\mathbf{Y}_E} V\left(\mathbf{X}, \mathbf{Y}_I, \mathbf{Y}_E, \mathbf{Y}_F\right) - M_S \gamma \dot{\mathbf{Y}}_E + \boldsymbol{f}_{\mathbf{Y}_E}(t)$$

- **with additional isotropic local frictional**

$$\gamma = \pi \omega_D / 6 = \pi k_B \theta_D / 6\hbar$$

and Gaussian white-noise type random forcing terms

$$\boldsymbol{f}_{\mathbf{Y}_E}(t) = (2\gamma k_B T M_S / h)^{1/2} \boldsymbol{\xi}_{\mathbf{Y}_E}$$

$$< \boldsymbol{f}_{\mathbf{Y}_E}(t)\, \boldsymbol{f}_{\mathbf{Y}_E}(0)^T >= 2\delta(t)\gamma M_S k_B T \overleftrightarrow{\mathbf{1}}$$

4. Fixed Zone ($\mathbf{V}_> \cup \bar{\mathbf{V}}_<$)

- **Unaffected by interaction**

3.1.2 Interaction Potential Model

- Incident AO – Material surfaces
- Interatomic potential on material surfaces

1. Incident AO/Material Surface

- **Base Potential**

$$V(r)=D_e^o\left[e^{2a(r_e-r)}-2e^{a(r_e-r)}\right]$$

- **Model I (For metals, crystalline and polyethylene materials)**

$$V(r)=\varepsilon_s D_e^o\left[e^{(\varepsilon_e r_e-r)/a}-2\varepsilon_{gs}e^{(\varepsilon_e r_e-r)/2a}\right]$$

ε_s - correction factor to account for the interaction of an AO with multi-particles on the material surface

ε_e - effective equilibrium-distance factor

ε_{gs} - weighting factor

- **Model II (For polyethylene materials)**

$$V(r) = D_e^o \left[e^{2a(\varepsilon_e r_e - r)} - 2\varepsilon_{gs} e^{a(\varepsilon_e r_e - r)} \right]$$

2. Effective Interatomic Potential

$$U'_{Lif} = -\frac{4}{\pi}\left(\frac{\varepsilon_\infty + 2}{3}\right)^2 \frac{3\hbar}{4R^6}\omega^0\alpha^2$$

3.1.3 Reaction Probability Model

$$P_R = \frac{N_R\left(r_c; E_i; \theta_k\right)}{N_T\left(r_c; E_i; \theta_k\right)}$$

N_R - No. reactive trajectories

N_T - No. total trajectories

θ_k - Incident angle of the incoming particle

- accommodation coefficients (nonreactive trajectories)

$$\alpha = \frac{\overline{E}i - \overline{E}f}{\overline{E}i - 2k_B T_s}$$

3.2 Numerical Procedure

- **Standard Verlet algorithm**

3.3 Some Numerical Results

- AO/graphite
- AO/polyethylene
- AO/Kapton

1. AO/graphite

- Miller index of the graphite surface: (100)
- Calculations uses: 105 inner atoms, 228 edge atoms, 2117 fixed atoms.
- Initial velocities: Maxwell-Boltzmann distribution for T=394K
- Debye temperature $\theta_D = 420K$
- Depth of the potential well

$$D_e^o = D_o^o + \frac{1}{2}\hbar\omega = 11.23eV$$

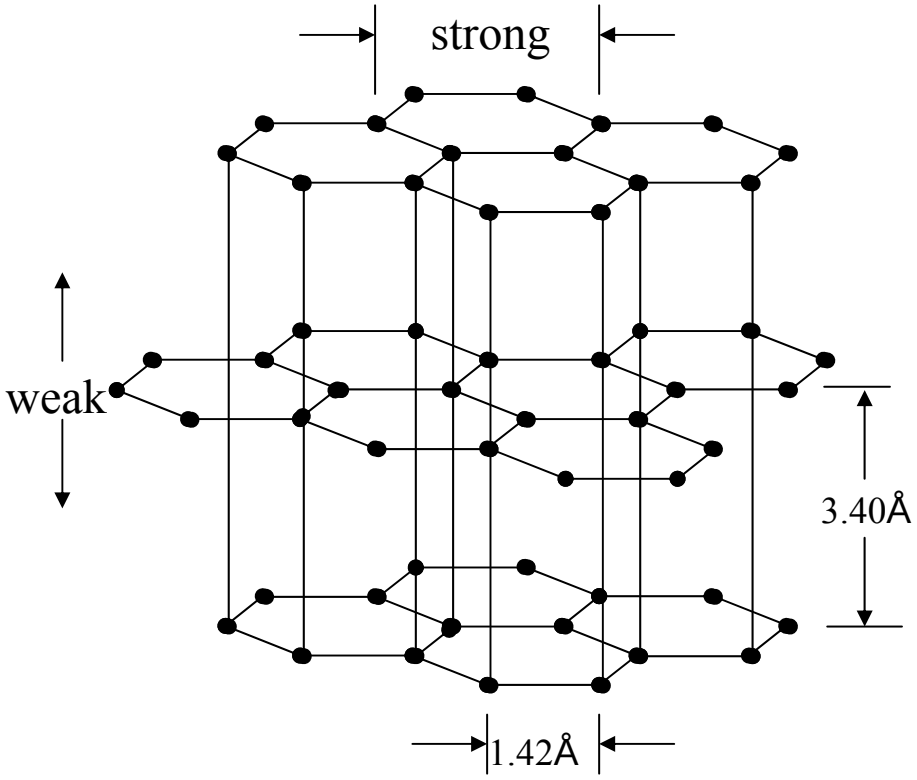

Reactive Probability for AO/Graphite

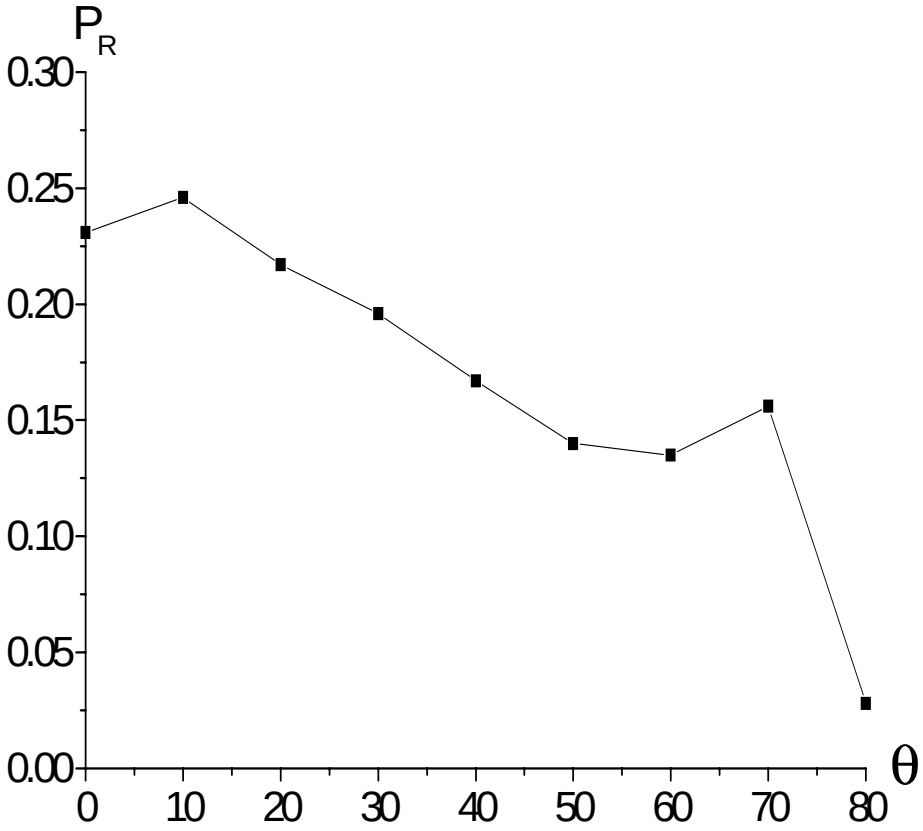

θ(deg.)	P_R	$\langle P_R \rangle$	P_{R-LEO}
0	0.231		(STS46)
10	0.246		
20	0.217		
30	0.196	0.168	0.125
40	0.167		
50	0.140		
60	0.135		
70	0.156		
80	0.028		

$\Delta P_R \sim 34\%$

Incident angle-dependence of reaction probability for $\varepsilon_s = 14$, $\varepsilon_{gs} = 0.3$

2. AO/polyethylene

- Miller index of the polyethylene surface: (100)
- Calculations uses: 50 inner repeat units
  97 edge repeat units
  867 fixed repeat units
- Initial velocities: Maxwell-Boltzmann distribution for T=310K
- Debye temperature θ_D = 218K
- Required reactive criterion = 0.686Å

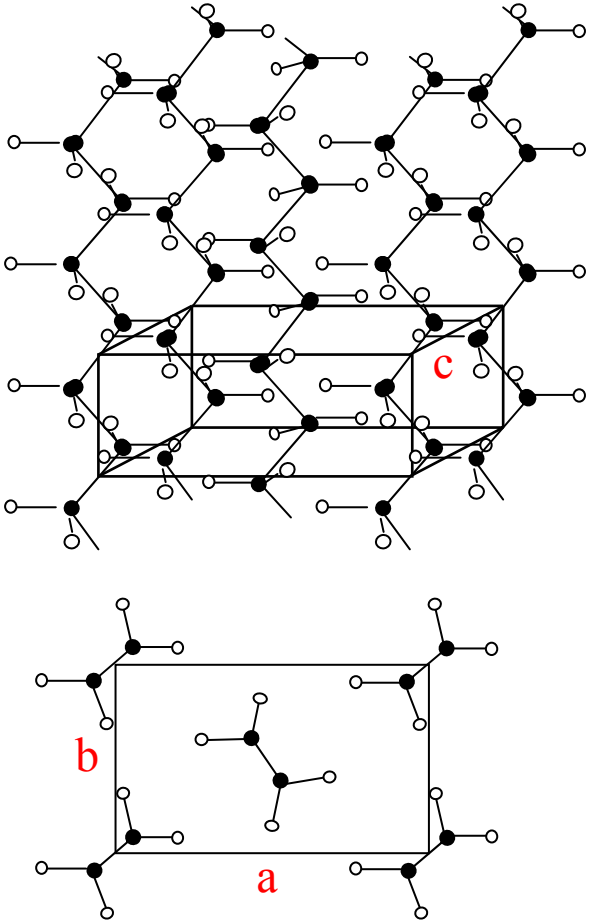

Reactive Probability and energy accommodation coefficient for

θ(deg.)	0	10	20	30	40	50	60	70	80
P_R	0.383	0.371	0.337	0.255	0.210	0.141	0.093	0.072	0.084
α	0.8816	0.8444	0.8452	0.7791	0.7553	0.6900	0.5913	0.4880	0.4581
$\langle P_R \rangle$	0.216								
$P_{R\text{-}LEO}$	0.189 (STS-46)								
$\langle \alpha \rangle$	0.6823								

$\Delta P_R \sim 14.3\%$

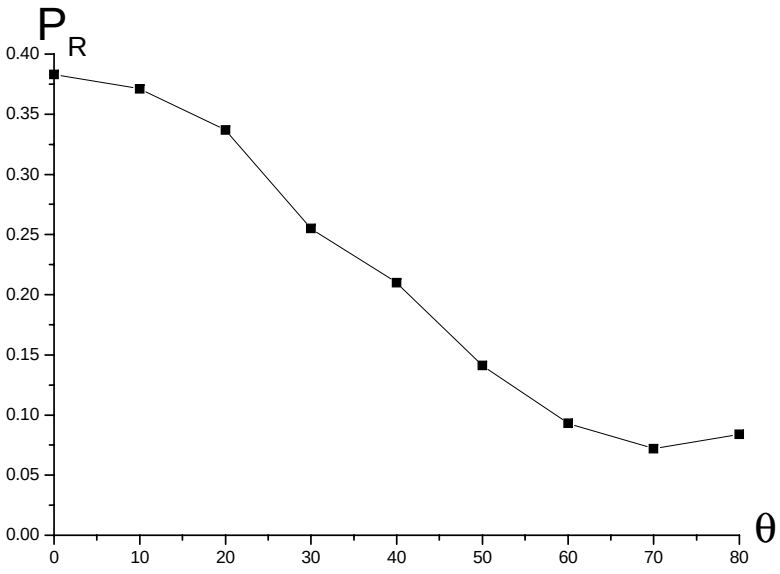

Incident angle-dependence of reaction probability

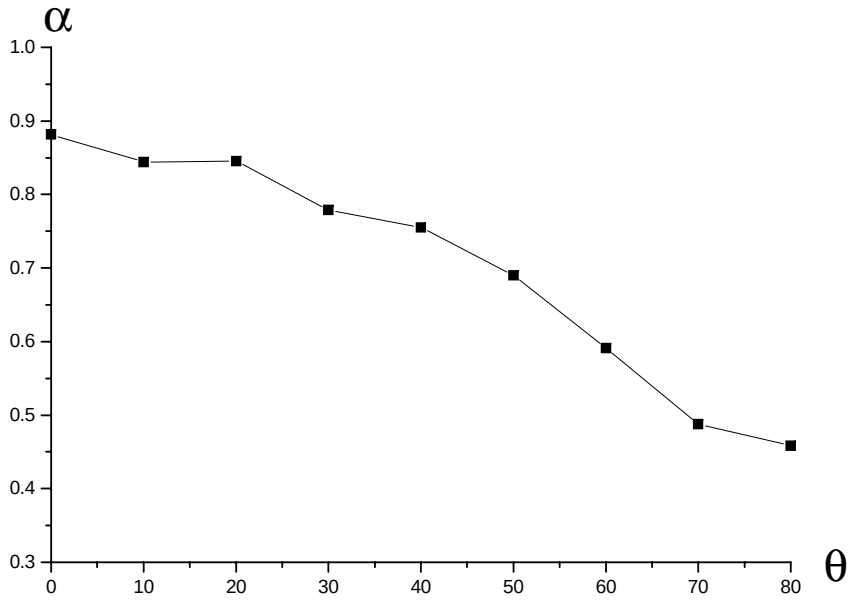

Incident angle-dependence of energy accommodation coefficient

$$\varepsilon_s = 3.0, \cdots \varepsilon_{gs} = 0.098, \quad \varepsilon_e r_e = 4.12\,\text{Å}$$

3. Kapton

- Miller index for the lattice surface of Kapton® : (100)
- Calculations:

  for $0^o \leq \theta \leq 70^o$

  394 inner- monomers
  897 edge-
  2579 fixed-

  for $\theta > 70^o$

  10 inner- monomers
  449 edge-
  3411 fixed-

- Initial velocities: Maxwell-Boltzmann distribution for T=310K
- Debye temperature $\theta_D = 165\ K$
- Required reactive criterion = 0.686Å

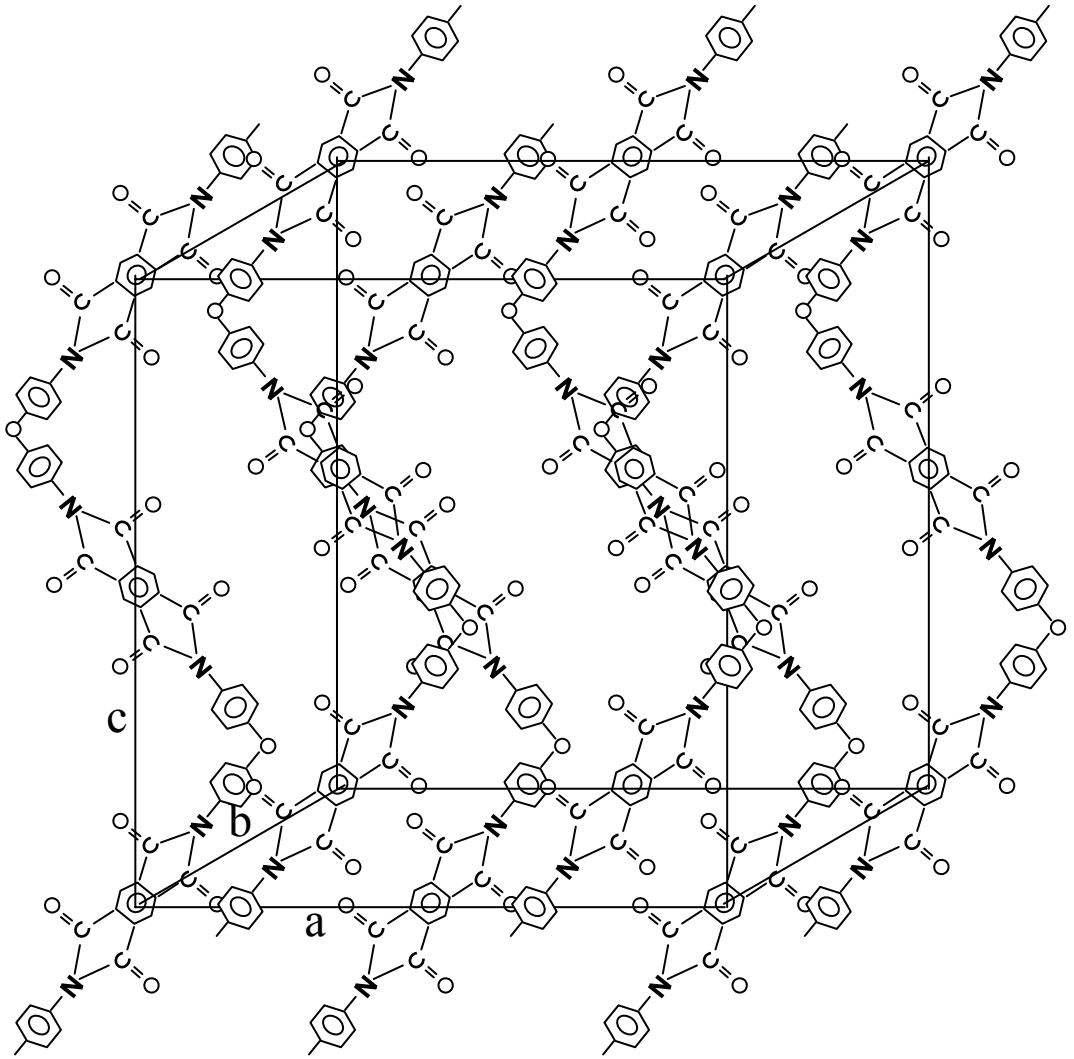

Reactive probabilities for different factors and STS-46 flight experiment

ε_e	2.9	3.0	3.0	3.0	3.0	2.9	3.1
ε_{gs}	0.2	0.2	0.25	0.35	0.68	0.0	0.2
θ (deg.)	P_R						
0	0.335	0.256	0.267	0.261	0.28	0.338	0.218
10	0.327	0.262	0.253	0.258	0.29	0.322	0.229
20	0.288	0.238	0.229	0.242	0.243	0.303	0.191
30	0.241	0.23	0.228	0.221	0.219	0.251	0.167
40	0.233	0.154	0.173	0.205	0.198	0.185	0.13
50	0.161	0.127	0.115	0.148	0.187	0.157	0.074
60	0.105	0.065	0.084	0.093	0.135	0.077	0.05
70	0.084	0.042	0.05	0.056	0.126	0.048	0.017
80	0.029	0.013	0.019	0.035	0.09	0.0	0.002
$\langle P_R \rangle$	0.2003	0.1541	0.1576	0.1688	0.1964	0.1868	0.1198
$P_{R\text{-}LEO}$	0.2409						

Incident angle-dependence of reaction probability coefficient

$\varepsilon_{gs} = 0.20, \quad \varepsilon_e = 2.9$

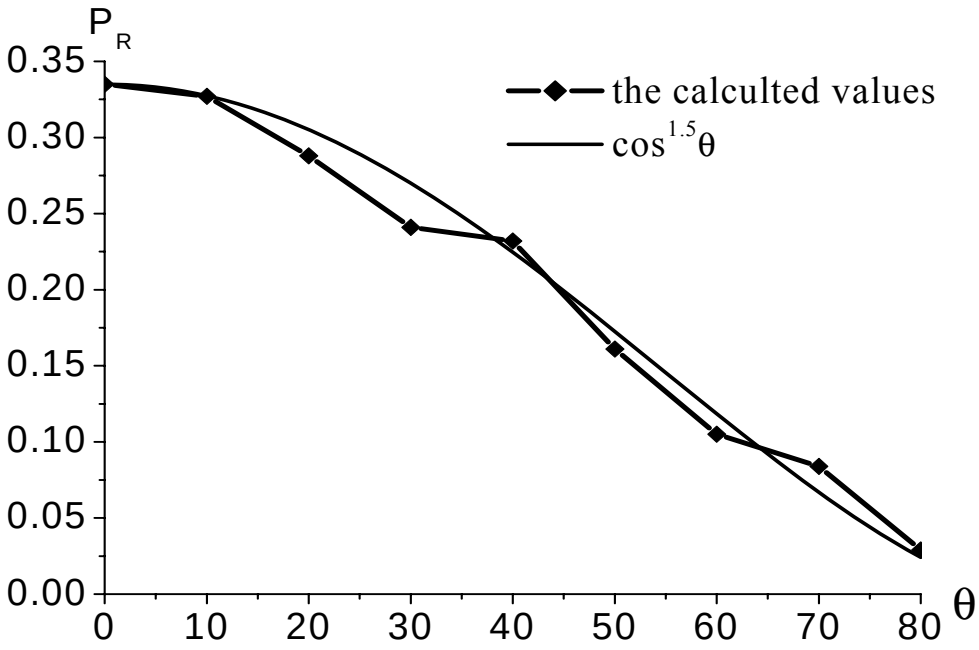

Incident angle-dependence of energy accommodation coefficient

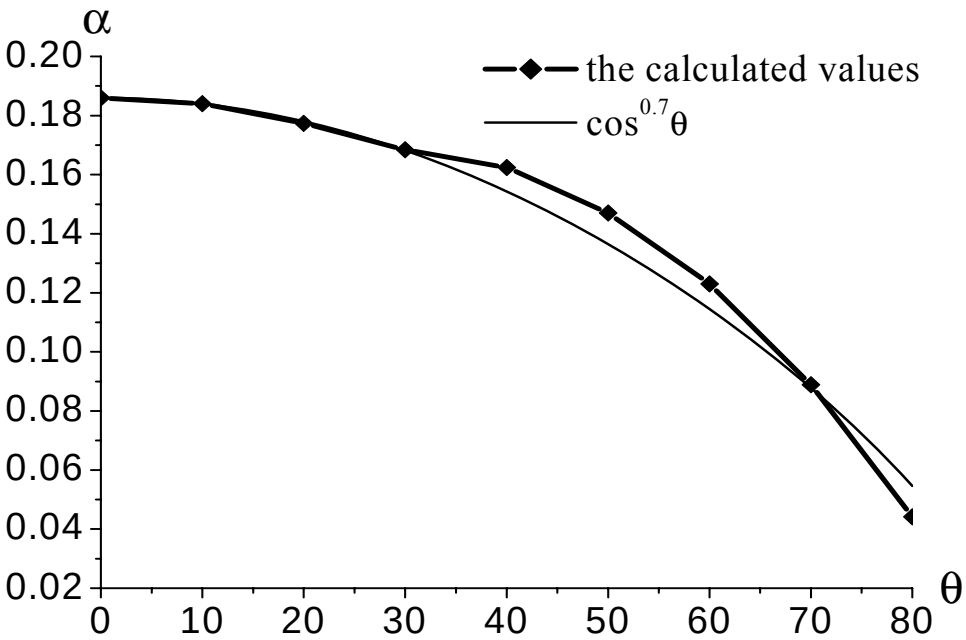

IV. Concluding Remarks

1. Conclusions:

- **Progresses**
  - experimental and theoretical analyses
  - crystalline materials (metals, nonmetals)
  - polymeric materials
  - effective interatomic potential – based meanfield theory
- **Difficulties**
  - More reliable interactive potentials are needed for diff. materials

    theoretical model + experimental measurements
  - Development of engineering models for evaluating the AO erosion of space materials

2. Undergoing Work

- **Experimental :**
  - protection material evaluation and selection
- **Theoretical:**
  - reaction-diffusion equation modeling
  - further study on interactive potential modeling

3. Future Work

- interactive potential modeling —— experimental + theoretical
- theoretical modeling of combined effects on AO+UV radiation

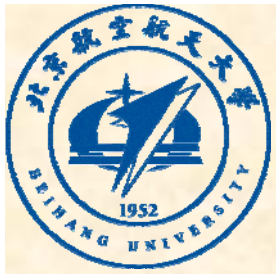

Thanks!